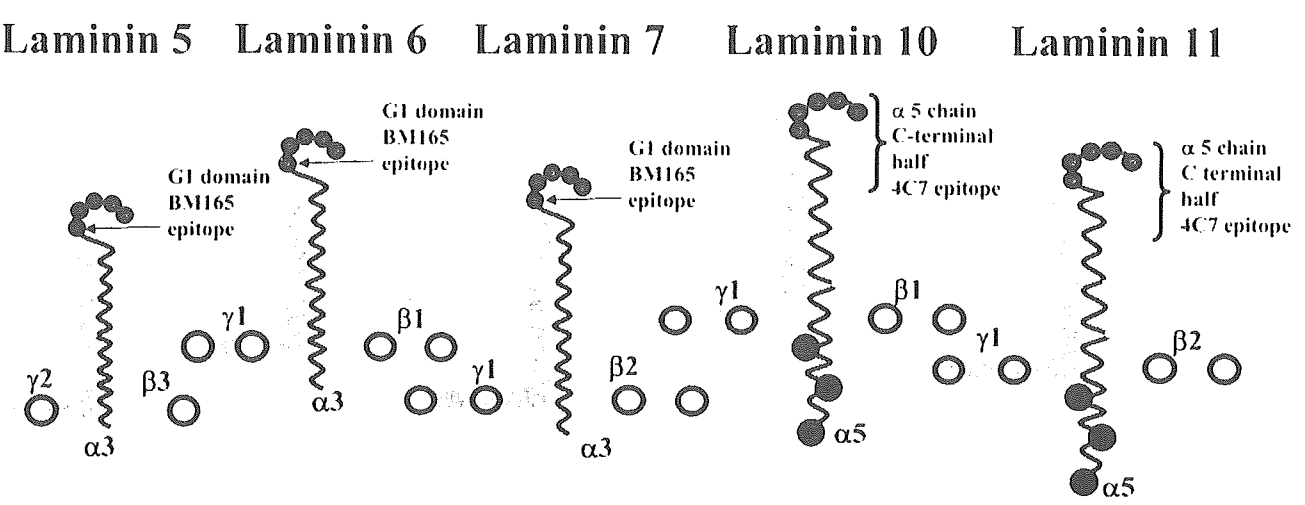

Figure 1 Schematic diagram showing the structure of laminin 5 and 10 chains and the position of two antibody binding sites in the α3 chain G1 domain (BM165) and the carboxyl terminal half of the α5 chain (4C7). This schematic diagram is not drawn to scale and does not include any α3 chain splice variants of laminin 5 (α3 β3 γ2). The antibody BM165 binds to the first globular (G1) domain of the α3 chain of laminins 5/6 (McMillan et al. 2003b), whereas the antibody 4C7 binds to the carboxyl terminal half end of the α5 chain (present in both laminins 10 and 11).

(Pouliot et al. 2002). However, in certain non-epithelial cells, the integrins α3β1, α6β1, and α6β4 and α dystroglycan are expressed and have been identified as possible laminin 10/11 receptors (Kikkawa et al. 1998, 2000; Yu and Talts 2003).

Antibodies are now available that recognize specific laminin chains and provide new tools to investigate the structure of the epidermal basement membrane. These antibodies include 4C7 (Engvall et al. 1990; Tiger et al. 1997) that recognizes a carboxyl terminal domain of the human α5 chain of laminins 10 (α5 β1 γ1, see Figure 1) and 11 (α5 β2 γ1). This antibody blocks the epitope involved in neurite cell adhesion to the laminin α5 chain (Engvall et al. 1986; Makino et al. 2002). Further laminin-specific antibodies to β and γ chains include 2E8 (recognizing the β1 chain (Engvall et al. 1986), D18 (γ1) (Sanes et al. 1990), and C4 (β2) (Hunter et al. 1989).

To better understand the position and possible functions of epidermal molecules, we examined the precise localization of the α5, β1, β2, and γ1 laminin chains and collagen IV in the interfollicular and follicular epidermal basement membrane. In addition, the expression of laminin chains was also assessed in a range of epidermolysis bullosa (EB) patients' skin harboring defects in several basement membrane components, including laminin 5. We have quantitatively analyzed and compared the localizations of laminin α5, β1, β2, and γ1 chains with that of laminin 5 (α3 β3 γ2) from our previously published data (McMillan et al. 2003b) and collagen IV. Comparison of α5, β1, β2, and γ1 chain expression with laminin 5, a well-studied HD-associated isoform, will determine a more precise localization for these laminin isoforms. Our data support the hypothesis that multiple laminin isoforms colocalize beneath HDs in normal and diseased epidermal basement membranes.

Materials and Methods

Skin Samples

Samples of adult and neonatal control skin from non-specialized sites (abdomen, arm, thigh, $n=8$; and scalp skin, $n=2$) were obtained from routine surgical procedures. Skin samples were frozen for cryostat sectioning or processed for post-embedding immunogold electron microscopy (IEM) as described below. In all cases, the biopsies were performed with the patient's or guardian's informed consent, with the relevant institutional approval for experiments handling human material, and in accordance with the Helsinki Declaration.

Skin samples from patients affected with a group of rare genodermatoses, EB, were included in this study ($n=15$, see Table 1). Details of the number of patients for each EB disease subtype, their age at biopsy, details of any identified mutations, or significant results of diagnostic antibody staining are listed, in addition to the results of their laminin antibody staining findings (see Table 1). Four Herlitz junctional (HJ) EB patients harbored laminin-5 chain mutations that were reported in the literature (Takizawa et al. 1998a–d). In one EB simplex associated with muscular dystrophy (EBS-MD) patient, genetic defects have been reported (Pulkkinen et al. 1996).

Confocal Immunofluorescence Microscopy

Indirect immunofluorescence was performed as previously described (Kennedy et al. 1985) using cryostat skin sections. Laminin chain expression was confirmed in control skin using the following antibodies: 4C7 recognizing the human α5 chain (see Figure 1) present in laminins 10 and 11 (dilution

Table 1 Comparison of laminin 5 and laminin 10 expression in patients with various forms of epidermolysis bullosa

EB disease subtype	Deficient protein	Patients' sex, age, mutation, and staining details	Laminin-5 γ3 chain GB3 expression	Laminin-10 α5 chain 4C7 expression
Control (5)	Normal	M/31 years, 33 years, 41 years, 45 years, F/15 years	+++	+++
HJEB (6)	Laminin 5	M/1 month, W610X/Q166X LAMB3	−	+/++
		F/9 months, 1997-2A>C (homozygous, LAMB3)		
		F/1 month, Q936X LAMB3		
		M/1 month, 1929delCA/W610X LAMB3		
		F/2 months, M/1 month, laminin-5 negative (GB3 moAb)		
NHJEB (2)	Laminin 5	M/12 years, M/5 years, laminin-5 reduced (GB3 moAb)	+	+++
NHJEB (2)	Collagen XVII	M/21 years, F/35 years, G252X collagen XVII negative (233, 1A8C moAb)	+++	+++
SRDEB (2)	Collagen VII	M/7 years, M/1 year, collagen VII negative (LH7:2 moAb)	+++	+++
JEB-PA/PA-EBS (1)	Integrin α6β4	F/1 month, α6β4 integrin negative (3E1,GOH3 moAb)	+++	+++
EBS-MD (2)	Plectin	M/27 years, M/9 years, plectin negative (HD1-121 moAb)	+++	+++

EB, epidermolysis bullosa; HJEB, Herlitz junction epidermolysis bullosa; NHJEB, non-Herlitz junctional epidermolysis bullosa; SRDEB, severe recessive dystrophic epidermolysis bullosa; JEB-PA, junctional epidermolysis bullosa associated with pyloric atresia; which is also known as EBS-PA, epidermolysis bullosa associated with pyloric atresia. +++, normal, bright staining pattern along dermal–epidermal junction; ++, reduced dermal–epidermal junction staining compared to controls; +, severely reduced dermal–epidermal junction staining compared to controls; −, absent dermal–epidermal junction staining compared to controls.

1:25; Chemicon International, Temecula, CA) (Engvall et al. 1990; Tiger et al. 1997). The monoclonal antibody 2E8 recognizing the β1 chain (neat) (Engvall et al. 1986), the monoclonal antibody D18 that recognizes the γ1 chain (see Figure 1) (neat) (Sanes et al. 1990), and an antibody C4 to the β2 chain (see Figure 1) (used neat) (Hunter et al. 1989) were also included. The antibodies 2E8, D18, and C4 were obtained from the Developmental Studies Hybridoma Bank, University of Iowa (Iowa City, IA). The mouse monoclonal M3F7 recognizing the helical domain of the α1 and α2 chains of collagen IV (used neat) (Foellmer et al. 1983) was also obtained from the Developmental Studies Hybridoma Bank. Laminin-5 antibodies included the mouse monoclonal BM165 directed against the laminin-5 α3 chain terminal first globular (G1) domain (see Figure 1) (diluted 1:50) (Marinkovich MP, unpublished data) (McMillan et al. 2003b); K140 directed against the laminin-5 β3 chain adjacent to domain IV; GB3 directed against the laminin-5 γ2 chain (Harlan Sera Lab; Loughborough, UK); and a rabbit polyclonal serum directed against the entire laminin-5 molecule (1:200) (McMillan et al. 2003b). The melanocyte marker antibody TMH-1 recognized the b-locus protein (rat antibody, 1:10 dilution) and was previously described by Masunaga et al. (1996).

Epidermal sections were fixed in cold acetone (−20C) for 10 min and incubated with 5% normal rabbit sera in 0.1 M Dulbecco's PBS for 5 min at 37C. Sections were incubated with primary antibodies and subsequently with secondary antibodies conjugated to fluorescein isothiocyanate or Texas Red (FITC; rabbit anti-mouse IgG or goat anti-rabbit IgG, 1:200; DAKO, Tokyo, Japan; Texas Red conjugated donkey anti-rabbit; Amersham, UK). To label TMH-1, a preabsorbed cyanine (CY5)-conjugated goat anti-rat antibody was used (Jackson ImmunoResearch; West Grove, PA). All secondary antibodies were diluted in 3% BSA in 0.1 M PBS for 30 min at 37C in a darkened, humidified chamber. Sections were then labeled with a ToPro-3 nuclear counterstain (diluted 1:20,000, blue channel; Jackson ImmunoResearch) if appropriate. The sections were then mounted in Permafluor (Thermo Shandon; Pittsburgh, PA) and examined with a confocal microscope (Fluoview FV300; Olympus, Tokyo, Japan) using an inverted microscope (IX70; Olympus). Controls included normal skin cryostat sections with the primary antibody substituted by PBS, myeloma supernatant, or an irrelevant immunoglobulin isotype, as a negative control. All experiments were performed at least in duplicate.

Immunogold Electron Microscopy

Four samples of human skin were cryofixed and processed for postembedding IEM according to the previously described methods (Shimizu et al. 1989,1990). Samples were washed in PBS and cryoprotected in 20% glycerol (in PBS) for up to 1 hr at 4C. Subsequently, cryofixation was performed in liquid propane at −190C using a freeze plunge apparatus (Leica CPC; Cambridge, UK) followed by freeze substitution over 3 days at −80C in methanol using an automated freeze substitution system (AFS; Leica). Specimens were embedded in Lowicryl K11M (Ladd Research Industries; Burlington, VT) resin over 4 days at −60C. The temperature was gradually raised and the resin was polymerized under UV light and liquid nitrogen vapor at 10C. Ultrathin sections were then cut and collected on pioloform-coated nickel grids. Sections were stained with uranyl acetate only (15 min) and observed with a transmission electron microscope (Hitachi H-7100; Tokyo, Japan) at 75 kV. Blocks showing good ultrastructure were selected for immunolabeling experiments. Sections were preincubated in buffer containing PBS with 5% normal goat serum (NGS), 1% BSA, and 0.1% gelatin. Primary antibodies or human antisera were all diluted in PBS buffer containing 1% NGS, 1% BSA, and 0.1% gelatin and incubated at 37C for 2 hr. The sections were then washed in a drop of PBS buffer four times (5 min each) and placed on a drop of secondary linker antibody, again diluted in PBS buffer (for 2 hr at 37C). The secondary antiserum, rabbit anti-mouse IgG (DAKO; Ely, UK) was diluted 1:500. Sections were then incubated with a final antibody layer using 5-nm gold-conjugated labeled goat anti-rabbit or goat anti-mouse antibodies (Biocell; Cardiff, UK) diluted 1:500 in Tris-buffered saline (TBS) for 2 hr at 37C. For double labeling on K11M sections, the α5 chain of laminins 10/11 (4C7 and a 5-nm

gold-conjugated goat anti-mouse) and rabbit anti-laminin 5 (polyclonal highlighted by 15-nm gold-conjugated goat anti-rabbit; Biocell) were used. Sections were washed twice in TBS buffer and twice in distilled water (5 min each). After staining with 15% alcoholic uranyl acetate (3 min) and lead citrate (15 min), sections were observed with a transmission electron microscope (H-7100; Hitachi). Controls included normal skin sections with the primary antibody substituted by PBS, myeloma supernatant, preimmune rabbit serum, or an irrelevant immunoglobulin isotype, as a negative control. All experiments were performed in triplicate.

Immunogold Quantitative Analysis

The techniques for ultrastructural labeling were similar to those performed by McMillan et al. (2003b). Electron micrographs were taken at a standard magnification (30K) and were enlarged by a standard factor ×2.08. The final magnification (×62,500) was checked using electron micrographs taken of a carbon diffraction grating. For standardization purposes, all observations were made by one observer (JRM). At least 200 gold particles were assessed per specimen for each antibody or antiserum and four specimens from different individuals were examined (see Table 1 and Table 2). A 5-nm immunogold-conjugated final antibody layer was used. The percentage of gold particles perpendicularly beneath an observable electron-dense HD cytoplasmic outer attachment plaque as described by McMillan and Eady (1996) was scored and calculated from a large number of gold particles in skin from four individuals.

Only non-obliquely sectioned areas of dermal–epidermal junction were included with clearly defined HD plaques, lamina lucida (LL), and lamina densa (LD). The dermal–epidermal junction beneath melanocytes or in damaged areas was excluded from this study. Gold particles that appeared clumped or associated with any deposit were excluded.

For each antibody or antisera, the positions of gold particles were statistically tested by one-way ANOVA and a two-sample *t*-test using the Minitab statistical package (Minitab Inc; University of Pennsylvania, Philadelphia, PA). An antibody (4C7) that recognizes a carboxyl terminal domain of the α5 chain of laminins 10/11 was used to determine the mean position of labeling directly beneath the keratinocyte plasma membrane (Engvall et al. 1986; Makino et al. 2002)(see Figure 1 for epitope position). The labeling of the α5 chain was compared with the distribution of the G1 domain of laminin-5 α3 chain (using data previously reported by McMillan et al. 2003b).

Results

Confocal Fluorescence Microscopy of Control Skin

Laminin-5 staining was restricted to the dermal–epidermal junction in control skin (data not shown). This was similar to the dermal–epidermal junction staining of α5 chain of laminins 10 (data not shown). Laminins 10 and 11 were also expressed in dermal blood vessels. Laminin 11 (as identified by the β2 chain) dermal–epidermal junction staining was present in adult control thigh and arm skin but was variable in other samples including scalp skin. Therefore, β2 chain expression appears to be distinct and independent from that of the α5 chain. Staining for the α5, β1, and γ1 chains was weaker in the adult dermal–epidermal junction than in blood vessels (data not shown), whereas dermal–epidermal junction staining was generally brighter in younger skin samples (<16 years, data not shown). This would appear to support a previous report of age-dependent expression of the laminin 10/11 chains (Pouliot et al. 2002).

Confocal fluorescence microscopy (Figures 2A–2C) showed that both laminin-5 and α5 chains are expressed in the dermal–epidermal junction of control interfollicular epidermis except for small gaps (white arrows in Figures 2A and 2B) beneath small isolated cells presumed to be melanocytes staining blue for the melanocyte marker, TMH-1 (Figures 2A and 2B) (Masunaga et al. 1996). These data suggest that laminin-10 chains are restricted to beneath keratinocytes and are not expressed beneath melanocytes.

A previous scalp skin and hair follicle immunohistochemical study (Akiyama et al. 1995) demonstrated a specific staining pattern for many HD and anchoring filament components, particularly laminin 5, which manifests as reduced staining around the lower hair bulb and a reemergence of staining over the dermal papilla region (Akiyama et al. 1995). We observed this

Table 2 Immunogold particle distribution shows the majority of laminin labeling is restricted to beneath the hemidesmosome (HD) plaque

Antibody/antisera	Recognizes chain and epitope	Present in which chain/isoform(s)	Number of skin samples	Frequency of gold particles under HDs % (±SD)
Laminin 5	All chains[a]	Lam 5[a]	2[a]	77–88[a]
BM-165	α3 chain	Lam 5/6	4	82.65 (±3.87)
4C7	α5 chain	Lam 10/11	4	84.3 (±3.89)
2E8	β1 chain	Lam 6/10	4	91.7 (±3.99)
C4	β2 chain	Lam 7/11	4	88.4 (±3.56)
D18	γ1 chain	Lam 6/7/10/11	4	92.0 (±2.65)
M3F7	Collagen IV	α1/α2 helical (IV)	4	61.3 (±3.05)

[a]Data from McMillan et al. 2003b and Masunaga et al. 1996.

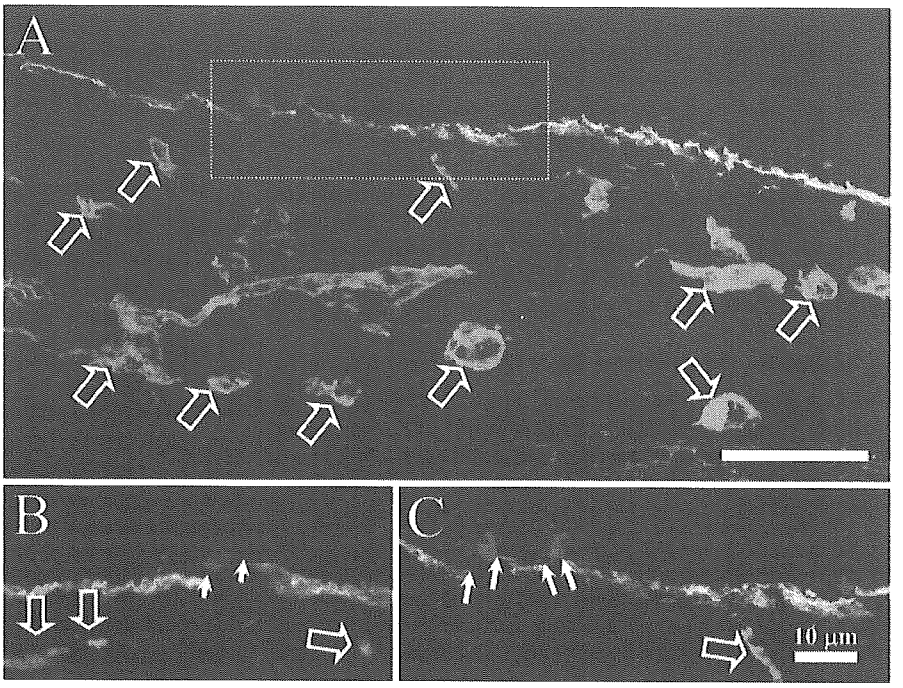

Figure 2 Reduced laminin 10 (green, FITC) and laminin 5 (red, Texas Red) labeling below the melanocyte marker TMH-1 (blue, CY-5) of normal adult control skin. Both laminin 5 and the α5 chain colocalize (orange color) within the dermal–epidermal junction (**A**) and both are expressed only weakly or are absent beneath melanocytes (**B,C**, in blue, see white arrows). The α5 chain of laminins 10/11 together with laminin 5 is not expressed beneath melanocytes (**A–C**, white arrows) but does show a distinct, strong expression pattern that includes dermal vessels (**A–C**, open arrows). Bar = 25 μm; Inset **C** = 10 μm.

characteristic pattern of staining along the majority of the follicles, for both laminin 5 (bracketed area in Figure 3A) and the laminin α5 chain (brackets and dotted line in Figures 3B and 3D). The laminin β1 and γ1 chains also showed this staining pattern (data not shown). There was no staining for the β2 chain in the hair follicle (data not shown). The dermal–epidermal junction of the bulge region stained for both α3 and the α5 chains (Figures 3A and 3B, Bu) and the α5 chain also stained the erector pili muscle (Figure 3C, EP).

Confocal Fluorescence Microscopy of Epidermolysis Bullosa Skin

The expression of laminins 5 (γ2 chain), 10 (all chains), and 11 (β2 chain) in patients with different forms of EB

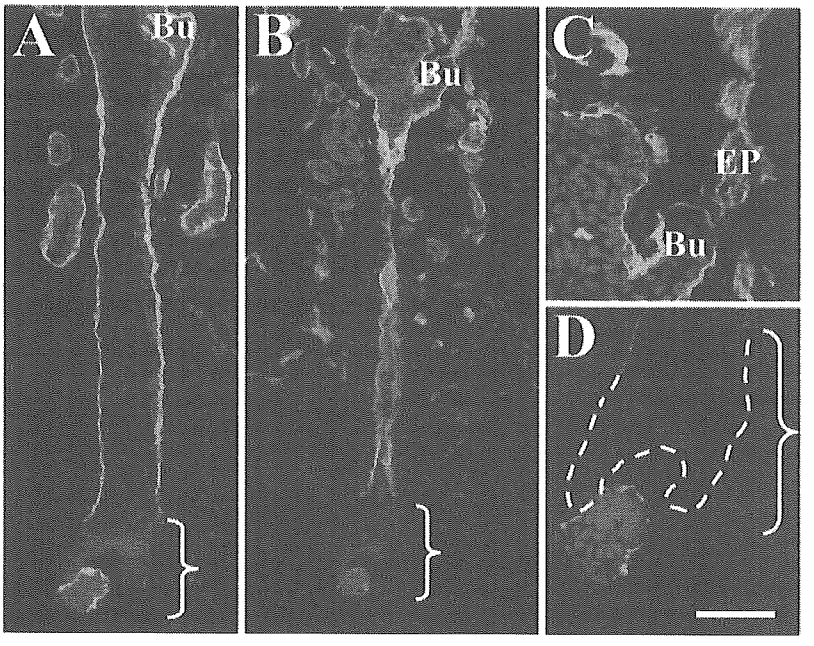

Figure 3 Indirect immunofluorescence shows a typical hemidesmosomal (HD) component-like expression pattern of the laminin α5 chain in late anagen human hair follicles. A previous scalp hair follicle immunohistochemical study (Akiyama et al. 1995) demonstrated a specific staining pattern for many HD-anchoring filament-associated components including laminin 5. In our study, both laminin-5 polyclonal staining (**A**) and the laminin α5 chain (**B**, 4C7) showed characteristic bright patterns along the epidermal proximal hair shaft including the bulge region (**B,C**, Bu) but progressively weaker staining toward the hair bulb (**D**, bracketed areas) with staining becoming brighter again higher up the hair shaft. Laminin α5 chain staining was present in the shaft (**B**) bulge region (**B,C**) and the apical tip of the hair bulb matrix (**D**). Laminin β1 and γ1 chains showed similar staining to the α5 chain (data not shown). No laminin β2 chain staining was detected in the hair follicle (data not shown). Bar = 25 μm.

was compared. In both control (Figure 4A) and all of the EB subtypes (Figures 4B–4H), α5, β1, β2, and γ1 chain expression was detectable. Laminin expression was weak in areas of split skin particularly in HJEB with defects in laminin 5 (α5 chain, Figures 4B and 4C, respectively, asterisks show the split area) (Uitto and Pulkkinen 2001). The reduction in α5 and β2 chain expression in HJEB patients, particularly over split skin,

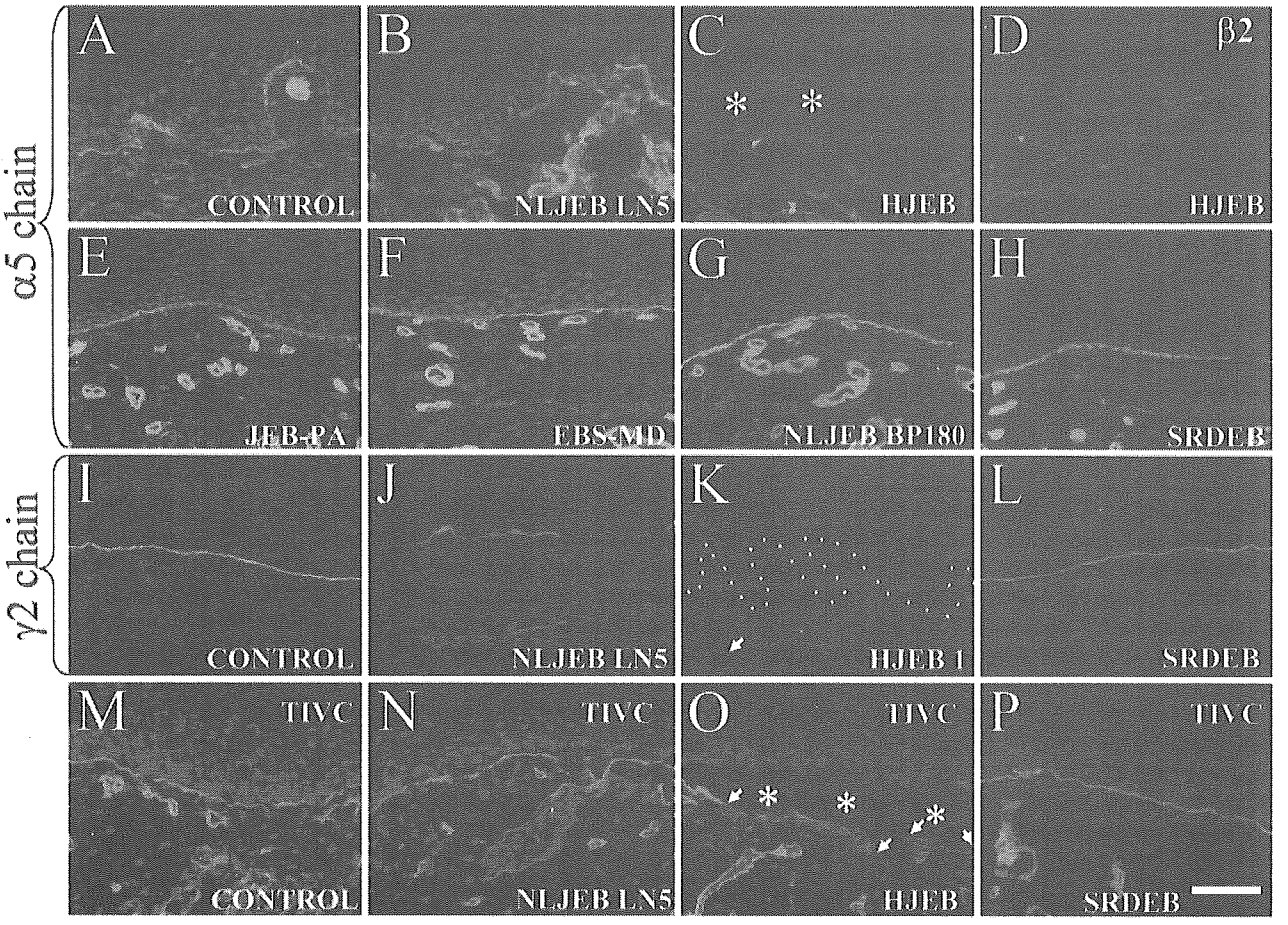

Figure 4 Laminin α5 and β2 chains are expressed beneath the epidermis in epidermolysis bullosa (EB) skin but are focally reduced in split lethal Herlitz junctional EB (HJEB) skin. The laminin α5 chain in control skin showed linear fluorescence along the dermal–epidermal junction and in dermal blood vessels (**A**). However, in non-lethal (**B**) and HJEB skin (**C,D**), the laminin α5 and β2 chains showed reductions in dermal–epidermal junction staining, especially where areas of skin had become separated (**C**, asterisks). This effect was due to antigen degradation in HJEB skin during skin separation as demonstrated by reduced collagen IV staining (**O**, arrows:) over the split areas (**O**, asterisks), whereas control skin (**M**), non-lethal junctional EB (NLJEB) (**N**) and dystrophic EB skin (**P**) showed bright linear collagen IV staining, respectively. The presence of α5 and β2 chain staining in intact EB skin demonstrates that these chains are independently synthesized and maintained even in the presence of other defective basement membrane components. All other cases of EB showed normal staining for the laminin α5 chain (and β2 chain, not shown), including junctional EB associated with pyloric atresia (JEB-PA with defects in α6β4 integrin (**E**), EB simplex associated with muscular dystrophy (EBS-MD with defects in plectin) (**F**), NLJEBBP180 with defects in BP180 (**G**), and severe recessive dystrophic EB (SRDEB with collagen VII defects (**H**). In control and SRDEB patients' skin, laminin-5 γ2 chains were normally expressed (**I** and **L**, respectively) using the γ2 chain monoclonal antibody GB3. Laminin-5 expression was severely reduced and absent in both the NLJEB and HJEB cases (**J,K**), respectively, harboring severe defects in laminin 5. Bar = 50 μm.

Figure 5 The majority of laminin 5 and laminin 10/11 chains are restricted to the lamina densa beneath HDs, whereas collagen IV is expressed continuously along the basal lamina. Postembedding immunoelectron microscopy with anti-α5 chain (laminin 10) (**A–D**) and double labeling with anti-α3 chain (laminin 5) (**E**) antibodies in control skin reveals a similar labeling pattern for these laminins. Collagen IV (M3F7), however, is not restricted to beneath HDs but is continuous along the basal lamina (**F**). Double labeling with laminin 5 polyclonal antiserum (15 nm gold particles) and laminin 10/11 (with smaller 5 nm gold particles) shows that the majority of labeling colocalizes beneath HDs at the border between the lamina lucida and lamina densa (**E**). The majority (84%) of laminin α5 chain labeling (see Table 2 and **A–D**) was restricted to areas immediately beneath the HDs, over the LD border (**A–D**, arrows) whereas only 61% of collagen IV was restricted to beneath HDs (**F**). HD plaques (solid arrows) are shown within the keratinocyte cytoplasm (white cross) and the lamina lucida highlighted by asterisks. Bar = 0.2 μm.

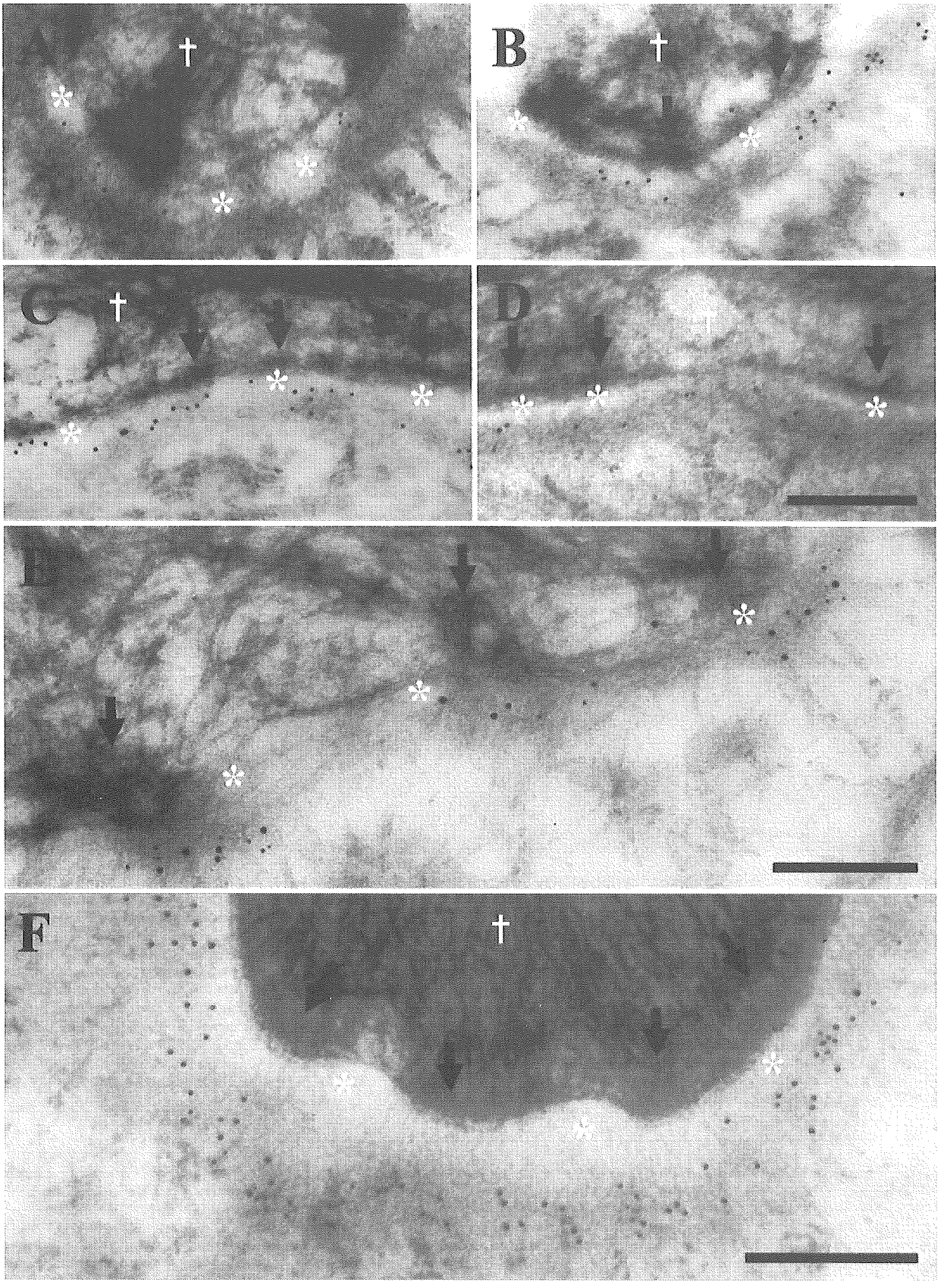

The Journal of Histochemistry & Cytochemistry

suggested that this effect might be due to antigen degradation in vivo in the split areas. The presence of α5 and β2 chains in intact EB skin, however, confirms that these chains are capable of being independently synthesized and assembled even in the total absence or in the presence of defective laminin 5. All other EB cases also showed normal staining for other laminins including junctional EB associated with pyloric atresia (JEB-PA) (with defects in α6β4 integrin, Figure 4E), EB simplex associated with muscular dystrophy (EBS-MD) (with defects in plectin, Figure 4F), non-lethal junctional (NLJEB) (with defects in BP180, Figure 4G), and severe recessive dystrophic epidermolysis bullosa (SRDEB) (Figure 4H). In control and SRDEB patients' skin there was normal staining for laminin 5 (γ2 chain using the antibody GB3, see Figure 4L). This was in contrast to laminin-5 chain staining that was severely reduced or absent in both the NLJEB (Figure 4J) and HJEB cases (Figure 4K), harboring severe defects in laminin-5 expression.

Immunogold Electron Microscopy and Quantitative Analysis

Labeling of control interfollicular epidermal sections showed that the majority of laminin-10 α5 chains (Figures 5A–5D; Table 2), β1, γ1, and 11 chain (β2 chain, data not shown) were restricted to under the cytoplasmic HD outer plaques. This was in contrast to collagen IV, which was not as restricted to beneath epidermal HDs plaques (see Figure 5F, 61% collagen IV vs 82% laminin 5). The difference between all laminin and collagen values was statistically significant using the one-way ANOVA ($p<0.001$) and Student's *t*-test ($p<0.000$). All four α5, β1, β2, and γ1 chain antibodies and antiserum showed a remarkable similarity in the percentage of labeling associated with the HD attachment plaque and anchoring filament complex beneath HDs, ranging between 84% and 92% (see Table 2). Furthermore, these values reflect an almost identical (HD restricted) expression pattern to the previously reported values for laminin-5 subunits (Masunaga et al. 1996; McMillan et al. 2003b) (part of these findings are also included in Table 2). Our data are very similar to those of laminin 5 (α3 chain) that on average demonstrated 82% of labeling restricted to beneath HDs (see Table 2) at a distance ranging from 35 to 45 nm below the plasma membrane at the LL–LD junction (Masunaga et al. 1996; McMillan et al. 2003b). The precise distance of the 4C7 epitope on the C-terminal portion of the α5 chain was 53.07 nm (±6.69 SD) from the plasma membrane (arrows, Figures 5A–5D). This is 18 nm lower than the G1 domain of the laminin-5 α3 chain described previously (see Figure 1) (McMillan et al. 2003b). The difference between these two α chain mean values was statistically significant using the one-way ANOVA ($p>0.01$) and Student's *t*-test ($p=0.009$). However, visual examination of the distribution of these two antigens revealed overlapping values ~30–40 nm beneath the plasma membrane, the only difference being that the α5 chain showed a wider range of labeling that extended deeper in the LD compared with the α3 chain. The remaining three β1-, β2-, and γ1-chain antibodies recognized, as yet unidentified, epitopes on specific laminin chains and were therefore not included in the plasma membrane distance measurements. However, all three antibodies showed upper LD labeling (not shown), the majority of which were restricted to beneath HDs similar to the α5 chain. The three β1-, β2-, and γ1-chain antibodies were excluded from the distance measurements but were scored for their localization either beneath visible HD attachment plaques (as defined by McMillan and Eady 1996) or within inter-HD areas.

Double labeling for the α5 chain of laminins 10/11 (highlighted by 5-nm small gold particles) and whole anti-laminin 5 antiserum (shown by the larger 15-nm gold particles) shows a similar labeling pattern in the LD beneath electron densities presumed to be HDs (Figure 5E). HD plaques are visible within the keratinocyte cytoplasm (white cross) and the dermal–epidermal junction is separated by the LL (Figure 5E, asterisks). Together our data suggest that the α5 chains (including β1, β2, and γ1 chains, see Table 2) show a restricted expression pattern beneath HDs, similar to laminin 5 but unlike collagen IV.

Discussion

We have demonstrated that the α5, β1, and γ1 chains show a similar localization to laminin 5 in the human interfollicular epidermal basement membrane. These data support the presence of multiple laminin isoforms beneath HDs in the basement membrane at several different epidermal sites. A very different localization of collagen IV within the LD but not restricted to beneath HDs was observed. These data suggest a complex network of interactions between different basement membrane components beneath the epidermis (Ghohestani et al. 2001; McMillan et al. 2003a; Miner and Yurchenco 2004).

In addition we have demonstrated that the expression of the α5 and β2 chains is independent of laminin 5, as demonstrated by residual staining in HJEB patients' skin. The reduction in α5 and β2 chain expression in HJEB was only observed over separated, blistered areas of skin, suggesting that this effect is due to separation-induced antigen degradation in vivo. This was supported by reduced collagen IV staining in split areas of EB skin. This was confirmed after reduced collagen IV staining was observed within separated areas of HJEB skin samples (data not shown). Our

results also suggest that the presence of other laminins cannot fully compensate for defects in laminin-5-deficient HJEB skin (McMillan et al. 1997,1998). The α5 and β2 chains were also normally expressed in all other EB samples harboring defects in plectin, collagen XVII (bullous pemphigoid antigen 2), the α6β4 integrin, and collagen VII.

In previous reports (Aumailley and Rousselle 1999), the laminin β2 chain was not expressed in the epidermal basement membrane of neonatal foreskin. However, we showed weak, variable β2 chain expression (in thigh and arm skin) and absences in other body sites (scalp skin). We conclude that the lack of β2 staining may be due to several factors: antigen masking, a low-level expression, or site- or age-specific variations in human laminin β2 chain expression that may include posttranslational protein processing seen in other laminin isoforms (Miner et al. 1997).

Laminin 5, together with several HD-associated antigens, is expressed in a specific pattern around late anagen hair follicles that excludes staining around the dermal papilla area (Akiyama et al. 1995; Nutbrown and Randall 1995). Laminin-10 chains also show this similar expression pattern in late anagen hair follicles. Unlike laminin-5 and laminin-10 chains, we failed to observe any β2 chain expression (laminins 7/11) in any part of the adult hair follicle; however, this may be due to a low level of antigen expression or masking of the β2 chain epitope. The significance of these findings may be related to the specific growth phases of the lower non-permanent portion of the hair follicle.

In the laminin α5 chain knockout mouse, an unusual disruption in hair follicle morphogenesis was demonstrated (Li, et al., 2003). Li et al. (2003) reported that, in control mice, laminin 10 was present in murine elongating hair germs when other laminins were down-regulated, suggesting a specific role for this laminin in hair follicle development and follicular keratinocyte migration. Mouse skin lacking laminin 10 also contained fewer hair germs and follicles compared with control mice, and after transplantation experiments this skin showed a failure of hair germ elongation and defective basement membrane assembly. Intriguingly, treatment of these mice with purified exogenous laminin 10 corrected these defects and restored hair follicle development. Given that human hair follicles are slow cycling and the majority remains in the late anagen phase and shows different growth characteristics to murine follicles, our failure to demonstrate such growth phase-specific differences in the expression of laminin 10 during the hair cycle stages is not surprising.

The presence of multiple laminin isoforms beneath HDs suggests the hypothesis that there are laminin subunits possibly with overlapping functions that form focal clusters of laminin molecules. This was in contrast to collagen IV, which was not restricted to HDs and localized to the LD region. Ultrastructural data show that the α3 chain (laminin 5) is closer to the plasma membrane than the α5 chain (with only an 18-nm difference, see Table 2). This might suggest that the α5 chain is more closely associated with a LD component such as collagen IV. However, given the size of both laminin chains of ~80–100 nm (as determined by rotary shadowing experiments), our data suggest a significant overlap occurs between α3 and α5 chains (Marinkovich et al. 1992; Vailly et al. 1994). Further studies using a larger battery of antibodies are required to determine the orientation of these laminin components.

Together these data show for the first time that laminin 10/11 chains are restricted to beneath HDs similar to laminin 5 but distinct from collagen IV. Our data suggest a specific localization of multiple laminin isoforms in the epidermal basement membrane beneath HDs and support the hypothesis that several laminins in close association may promote stable cell attachment among different basement membrane molecules.

Acknowledgments

This work was supported by a grant-in-aid of Scientific Research A (13357008, HS) and Health and Labor Sciences Research Grants (Research into Specific Diseases) H13-Saisei-02 and H17-Saisei 12, by a grant from the Japanese Society for the Promotion of Science (JSPS) grant #00345 to J.R.M., and by a grant-in-aid for JSPS fellows' research expenses (#00345). This work was also supported by a grant from the Japanese Health Science Foundation for Research Residents, for class "A" researchers (JRM).

We gratefully acknowledge the technical support of Ms. M. Sato and Ms. K. Sakai in this study. We also thank Dr. T. Masunaga for kindly providing the data from the γ2 chain study (Masunaga et al. 1996) and Dr. M.P. Marinkovich for his kind gift of his polyclonal laminin 5 antibody. Hybridoma supernatants D18 and 2E8 (produced by Drs. J. Sanes and E. Engvall) and M3F7 (from Dr. H. Furthmeyer) were obtained from the Developmental Studies Hybridoma Bank, developed under the auspices of the National Institute of Child Health and Human Development (NICHD) and maintained by the University of Iowa, Department of Biological Sciences, Iowa City, Iowa.

Literature Cited

Akiyama M, Dale BA, Sun TT, Holbrook KA (1995) Characterization of hair follicle bulge in human fetal skin: the human fetal bulge is a pool of undifferentiated keratinocytes. J Invest Dermatol 105: 844–850

Aumailley M, Rousselle P (1999) Laminins of the dermo-epidermal junction. Matrix Biol 18:19–28

Engvall E, Davis GE, Dickerson K, Ruoslahti E, Varon S, Manthorpe M (1986) Mapping of domains in human laminin using monoclonal antibodies: localization of the neurite-promoting site. J Cell Biol 103:2457–2465

Engvall E, Earwicker D, Haaparanta T, Ruoslahti E, Sanes JR (1990) Distribution and isolation of four laminin variants; tissue restricted distribution of heterotrimers assembled from five different subunits. Cell Regul 1:731–740

Foellmer HG, Madri JA, Furthmayr H (1983) Methods in laboratory investigation. Monoclonal antibodies to type IV collagen: probes

for the study of structure and function of basement membranes. Lab Invest 48:639–649
Geuijen CA, Sonnenberg A (2002) Dynamics of the α6β4 integrin in keratinocytes. Mol Biol Cell 13:3845–3858
Ghohestani RF, Li K, Rousselle P, Uitto J (2001) Molecular organization of the cutaneous basement membrane zone. Clin Dermatol 19:551–562
Gu J, Sumida Y, Sanzen N, Sekiguchi K (2001) Laminin-10/11 and fibronectin differentially regulate integrin-dependent Rho and Rac activation via p130(Cas)-CrkII-DOCK180 pathway. J Biol Chem 276:27090–27097
Hunter DD, Shah V, Merlie JP, Sanes JR (1989) A laminin-like adhesive protein concentrated in the synaptic cleft of the neuromuscular junction. Nature 338:229–234
Kennedy AR, Heagerty AH, Ortonne JP, Hsi BL, Yeh CJ, Eady RA (1985) Abnormal binding of an anti-amnion antibody to epidermal basement membrane provides a novel diagnostic probe for junctional epidermolysis bullosa. Br J Dermatol 113:651–659
Kikkawa Y, Sanzen N, Fujiwara H, Sonnenberg A, Sekiguchi K (2000) Integrin binding specificity of laminin-10/11: laminin-10/11 are recognized by α3β1, α6β1 and α6β4 integrins. J Cell Sci 113:869–876
Kikkawa Y, Sanzen N, Sekiguchi K (1998) Isolation and characterization of laminin-10/11 secreted by human lung carcinoma cells. Laminin-10/11 mediates cell adhesion through integrin α3β1. J Biol Chem 273:15854–15859
Li J, Tzu J, Chen Y, Zhang YP, Nguyen NT, Gao J, Bradley M, et al. (2003) Laminin-10 is crucial for hair morphogenesis. EMBO J 22: 2400–2410
Makino M, Okazaki I, Kasai S, Nishi N, Bougaeva M, Weeks BS, Otaka A, et al. (2002) Identification of cell binding sites in the laminin α5-chain G domain. Exp Cell Res 277:95–106
Marinkovich MP, Lunstrum GP, Burgeson RE (1992) The anchoring filament protein kalinin is synthesized and secreted as a high molecular weight precursor. J Biol Chem 267:17900–17906
Masunaga T, Shimizu H, Ishiko A, Tomita Y, Aberdam D, Ortonne JP, Nishikawa T (1996) Localization of laminin-5 in the epidermal basement membrane. J Histochem Cytochem 44:1223–1230
McMillan JR, Akiyama M, Shimizu H (2003a) Epidermal basement membrane zone components: ultrastructural distribution and molecular interactions. J Dermatol Sci 31:169–177
McMillan JR, Akiyama M, Shimizu H (2003b) Ultrastructural orientation of laminin 5 in the epidermal basement membrane: an updated model for basement membrane organization. J Histochem Cytochem 51:1299–1306
McMillan JR, Eady RA (1996) Hemidesmosome ontogeny in digit skin of the human fetus. Arch Dermatol Res 288:91–97
McMillan JR, McGrath JA, Pulkkinen L, Kon A, Burgeson RE, Ortonne J-P, Meneguzzi G, et al. (1997) Immunohistochemical analysis of skin in junctional epidermolysis bullosa using laminin 5 chain specific antibodies is of limited value in predicting the underlying gene mutation. Br J Dermatol 136:817–822
McMillan JR, McGrath JA, Tidman MJ, Eady RA (1998) Hemidesmosomes show abnormal association with the keratin filament network in junctional forms of epidermolysis bullosa. J Invest Dermatol 110:132–137
Mercurio AM, Rabinovitz I, Shaw LM (2001) The α6β4 integrin and epithelial cell migration. Curr Opin Cell Biol 13:541–545
Miner JH, Patton BL, Lentz SI, Gilbert DJ, Snider WD, Jenkins NA, Copeland NG, et al. (1997) The laminin α chains: expression, developmental transitions, and chromosomal locations of α1–5, identification of heterotrimeric laminins 8–11, and cloning of a novel α3 isoform. J Cell Biol 137:685–701
Miner JH, Yurchenco PD (2004) Laminin functions in tissue morphogenesis. Annu Rev Cell Dev Biol 20:255–284
Niessen CM, Hogervorst F, Jaspars LH, de Melker AA, Delwel GO, Hulsman EH, Kuikman I, et al. (1994) The α6β4 integrin is a receptor for both laminin and kalinin. Exp Cell Res 211:360–367
Nishiyama T, Amano S, Tsunenaga M, Kadoya K, Takeda A, Adachi E, Burgeson RE (2000) The importance of laminin 5 in the dermal-epidermal basement membrane. J Dermatol Sci 24(suppl 1): S51–59
Nutbrown M, Randall VA (1995) Differences between connective tissue-epithelial junctions in human skin and the anagen hair follicle. J Invest Dermatol 104:90–94
Pouliot N, Saunders NA, Kaur P (2002) Laminin 10/11: an alternative adhesive ligand for epidermal keratinocytes with a functional role in promoting proliferation and migration. Exp Dermatol 11: 387–397
Pulkkinen L, Smith FJ, Shimizu H, Murata S, Yaoita H, Hachisuka H, Nishikawa T, et al. (1996) Homozygous deletion mutations in the plectin gene (PLEC1) in patients with epidermolysis bullosa simplex associated with late-onset muscular dystrophy. Hum Mol Genet 5:1539–1546
Sanes JR, Engvall E, Butkowski R, Hunter DD (1990) Molecular heterogeneity of basal laminae: isoforms of laminin and collagen IV at the neuromuscular junction and elsewhere. J Cell Biol 111: 1685–1699
Shimizu H, McDonald JN, Gunner DB, Black MM, Bhogal B, Leigh IM, Whitehead PC, et al. (1990) Epidermolysis bullosa acquisita antigen and the carboxy terminus of type VII collagen have a common immunolocalization to anchoring fibrils and lamina densa of basement membrane. Br J Dermatol 122:577–585
Shimizu H, McDonald JN, Kennedy AR, Eady RAJ (1989) Demonstration of intra- and extra-cellular localization of bullous pemphigoid antigen using cryofixation and freeze substitution for postembedding immuno-electron microscopy. Arch Dermatol Res 281:443–448
Takizawa Y, Pulkkinen L, Shimizu H, Lin L, Hagiwara S, Nishikawa T, Uitto J (1998a) Maternal uniparental meroisodisomy in the LAMB3 region of chromosome 1 results in lethal junctional epidermolysis bullosa. J Invest Dermatol 110:828–831
Takizawa Y, Shimizu H, Pulkkinen L, Hiraoka Y, McGrath JA, Suzumori K, Aiso S, et al. (1998b) Novel mutations in the LAMB3 gene shared by two Japanese unrelated families with Herlitz junctional epidermolysis bullosa, and their application for prenatal testing. J Invest Dermatol 110:174–178
Takizawa Y, Shimizu H, Pulkkinen L, Nonaka S, Kubo T, Kado Y, Nishikawa T, et al. (1998c) Novel premature termination codon mutations in the laminin γ2-chain gene (LAMC2) in Herlitz junctional epidermolysis bullosa. J Invest Dermatol 111:1233–1234
Takizawa Y, Shimizu H, Pulkkinen L, Suzumori K, Kakinuma H, Uitto J, Nishikawa T (1998d) Combination of a novel frameshift mutation (1929delCA) and a recurrent nonsense mutation (W610X) of the LAMB3 gene in a Japanese patient with Herlitz junctional epidermolysis bullosa, and their application for prenatal testing. J Invest Dermatol 111:1239–1241
Tiger CF, Champliaud MF, Pedrosa-Domellof F, Thornell LE, Ekblom P, Gullberg D (1997) Presence of laminin α5 chain and lack of laminin α1 chain during human muscle development and in muscular dystrophies. J Biol Chem 272:28590–28595
Uitto J, Pulkkinen L (2001) Molecular genetics of heritable blistering disorders. Arch Dermatol 137:1458–1461
Vailly J, Verrando P, Champliaud MF, Gerecke D, Wagman DW, Baudoin C, Aberdam D, et al. (1994) The 100-kDa chain of nicein/kalinin is a laminin B2 chain variant. Eur J Biochem 219: 209–218
Yu H, Talts JF (2003) β1 Integrin and α-dystroglycan binding sites are localized to different laminin-G-domain-like (LG) modules within the laminin α5 chain G domain. Biochem J 371:289–299

Mutations in lipid transporter ABCA12 in harlequin ichthyosis and functional recovery by corrective gene transfer

Masashi Akiyama,[1] Yoriko Sugiyama-Nakagiri,[1] Kaori Sakai,[1] James R. McMillan,[2] Maki Goto,[1] Ken Arita,[1] Yukiko Tsuji-Abe,[1] Nobuko Tabata,[3] Kentaro Matsuoka,[4] Rikako Sasaki,[5] Daisuke Sawamura,[1] and Hiroshi Shimizu[1]

[1]Department of Dermatology, Hokkaido University Graduate School of Medicine, Sapporo, Japan. [2]Creative Research Initiative Sousei, Hokkaido University, Sapporo, Japan. [3]Division of Dermatology, Japanese Red Cross Sendai Hospital, Yagiyama, Tashiro, Sendai, Japan. [4]Division of Pathology and [5]Division of Dermatology, National Center for Child Health and Development, Okura, Setagaya, Tokyo, Japan.

Harlequin ichthyosis (HI) is a devastating skin disorder with an unknown underlying cause. Abnormal keratinocyte lamellar granules (LGs) are a hallmark of HI skin. ABCA12 is a member of the ATP-binding cassette transporter family, and members of the ABCA subfamily are known to have closely related functions as lipid transporters. ABCA3 is involved in lipid secretion via LGs from alveolar type II cells, and missense mutations in *ABCA12* have been reported to cause lamellar ichthyosis type 2, a milder form of ichthyosis. Therefore, we hypothesized that HI might be caused by mutations that lead to serious ABCA12 defects. We identify 5 distinct *ABCA12* mutations, either in a compound heterozygous or homozygous state, in patients from 4 HI families. All the mutations resulted in truncation or deletion of highly conserved regions of ABCA12. Immunoelectron microscopy revealed that ABCA12 localized to LGs in normal epidermal keratinocytes. We confirmed that ABCA12 defects cause congested lipid secretion in cultured HI keratinocytes and succeeded in obtaining the recovery of LG lipid secretion after corrective gene transfer of *ABCA12*. We concluded that ABCA12 works as an epidermal keratinocyte lipid transporter and that defective ABCA12 results in a loss of the skin lipid barrier, leading to HI. Our findings not only allow DNA-based early prenatal diagnosis but also suggest the possibility of gene therapy for HI.

Introduction

During the evolutionary process, when our ancestors left the safety of the aquatic environment, they developed a robust, protective mechanism or process in the skin that allowed adjustment to the new, dry environment; this is now known as keratinization. In humans, congenital defects involving skin keratinization cause a unique genodermatosis, ichthyosis (1, 2), which was named after the Greek word *ichthys*, meaning *fish*. Among the variety of types of ichthyosis, harlequin ichthyosis (HI) (Mendelian Inheritance of Man [MIM] 242500) is the most serious subtype (Figure 1); it is also the most severe congenital skin disorder of unknown etiology.

ABCA12 belongs to a large superfamily of ATP-binding cassette (ABC) transporters, which aid in the transport of various biomolecules across the cell membrane (3–5). The ABCA subfamily is thought to be important in lipid transport (6). ABCA12 is phylogenetically related to ABCA3, which is essential for alveolar surfactant lipid transport/secretion by lamellar granules (LGs) in type II alveolar lung cells. In skin, LGs are the most common secretory granules present in upper epidermal keratinocytes (7). Abnormal LGs are the most obvious characteristic findings in HI lesional epidermis. Furthermore, relatively minor missense mutations in *ABCA12* have been reported to underlie type 2 lamellar ichthyosis (MIM 601277), a milder form of ichthyosis (8). Thus, we hypothesized that *ABCA12* mutations leading to serious ABCA12 protein defects might underlie HI.

In the present study, we demonstrate that ABCA12 works as an epidermal keratinocyte lipid transporter and that defective ABCA12 results in a loss of the skin lipid barrier, leading to HI. We have found 5 distinct truncation, deletion, or splice-site mutations in 4 independent HI families. These mutations were present on both alleles of our HI patients, either in compound heterozygous or homozygous state. We demonstrate that *ABCA12* mRNA is expressed in normal human keratinocytes and that this expression is upregulated during keratinization. Our immunoelectron microscopic findings showed that ABCA12 protein localizes to LGs in the upper epidermal keratinocytes of human skin. Ultrastructural and immunofluorescent examination of human skin and cultured epidermal keratinocytes from HI patients who harbor *ABCA12* mutations revealed defective lipid secretion of LG lipid contents. In addition, using *ABCA12* corrective gene transfer in cultured HI keratinocytes, we have succeeded in restoring the normal ability of HI cells to secrete LG lipid.

Results

ABCA12 expression and localization in epidermal keratinocytes. To confirm the expression of *ABCA12* mRNA in human epidermal keratinocytes, we performed semiquantitative RT-PCR assays and demonstrated strong expression of *ABCA12* transcripts in cultured normal epidermal keratinocytes. To investigate the upregulation of *ABCA12* during keratinization under high-Ca^{2+} conditions, we evaluated the *ABCA12* transcript population against the GAPDH transcript using real-time RT-PCR. Calculation of the expres-

Nonstandard abbreviations used: ABC, ATP-binding cassette; CT, threshold cycle; HI, harlequin ichthyosis; LG, lamellar granule; MIM, Mendelian Inheritance of Man.

Conflict of interest: The authors have declared that no conflict of interest exists.

Citation for this article: *J. Clin. Invest.* 115:1777–1784 (2005). doi:10.1172/JCI24834.

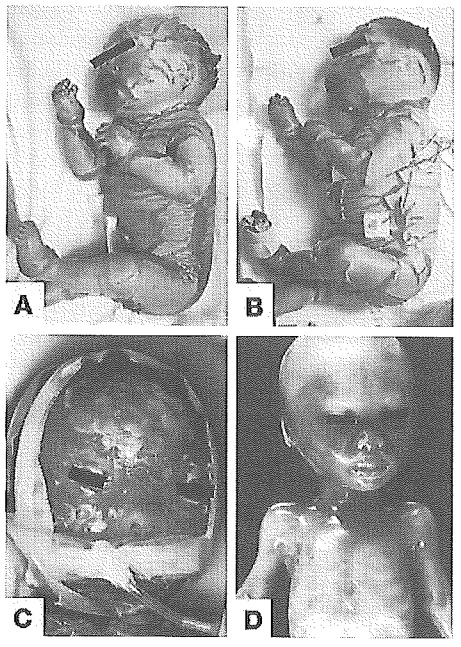

Figure 1
Clinical features of HI patients. (**A**) Patient 1 from family A harboring a homozygous mutation IVS23-2A→G in *ABCA12*. (**B**) Patient 2 from family B with compound heterozygous *ABCA12* mutations, IVS23-2A→G and 5848C→T (R1950X). (**C**) Patient 3 (family C) carrying compound heterozygous *ABCA12* mutations, 2021_2022del AA and 4158_4160delTAC (T1387del). (**D**) An affected fetus from family C aborted at 23 weeks' gestation showed no serious symptoms, although some abnormal keratinization was observed mainly on the cheeks and the perioral area.

sion ratios showed that *ABCA12* transcription was upregulated 4-fold after 1 week in high-Ca^{2+} culture. Furthermore, to confirm the expression of ABCA12 protein in the epidermis, we raised a polyclonal anti-ABCA12 antibody that recognizes an epitope near the C terminus of the ABCA12 polypeptide (residues 2567–2580) and performed immunostaining for ABCA12. ABCA12 was positive in the upper epidermal layers, mainly the granular layers, of normal human skin (Figure 2A); in contrast, there was an absence of immunolabeling in epidermal keratinocytes from HI patient 4 (Figure 2B), who harbors the homozygous truncation mutation R434X (see below). This mutation resulted in truncation of the protein, leading to loss of the epitope for the anti-ABCA12 antibody. These findings confirmed specificity of the anti-ABCA12 antibody. In the epidermis of patient 1, who harbors a homozygous splice acceptor site mutation IVS23-2A→G (see below), weak ABCA12 immunostaining was seen in the granular layer keratinocytes (Figure 2C). Immunoelectron microscopy revealed that ABCA12 protein was restricted to the LGs in the cytoplasm of epidermal keratinocytes (Figure 2, D and E). ABCA12-positive LGs were abundant close to the cell membrane and were observed fusing with the cell membrane to secrete their lipid content to the extracellular space of the stratum corneum (Figure 2F). These results indicate that ABCA12 is expressed in keratinocytes during keratinization and is likely to be involved in lipid transport into the extracellular space via LGs to form the stratum corneum lipid barrier (Figure 2G).

ABCA12 mutations in HI families. Full-length ABCA12 protein comprises 2595 amino acids and includes 2 ABCs containing 3 characteristic, highly conserved motifs (Walker A, Walker B, and active transport signature). In addition, there are 2 transmembrane domains, each consisting of 6 hydrophobic membrane-spanning helices. Mutational analysis of the 53 exons, including the exon-intron boundaries of the entire *ABCA12* gene, revealed 5 novel, distinct mutations in both alleles, either in compound heterozygous

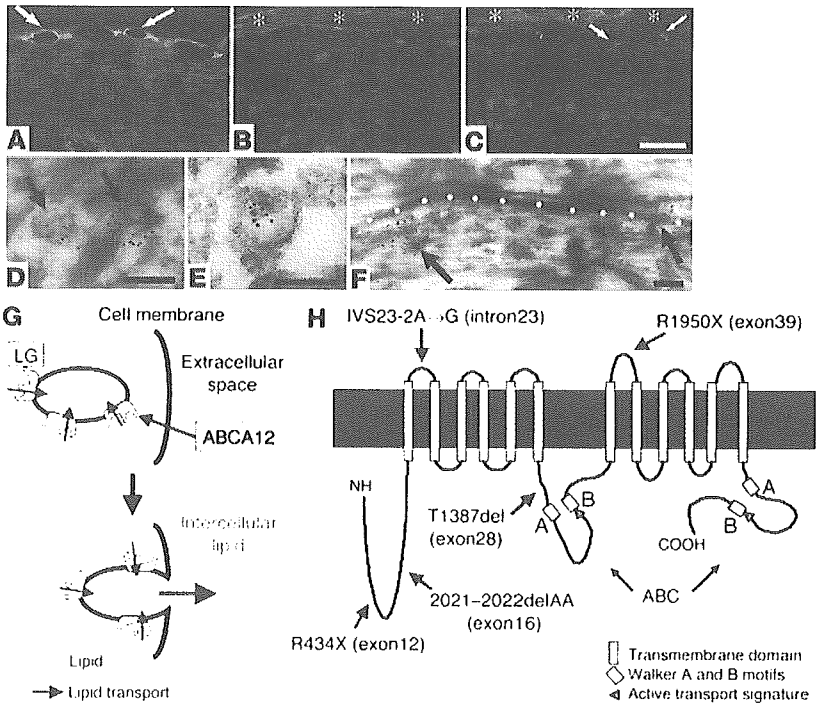

Figure 2
Localization and structure of ABCA12 protein and the sites of HI mutations. (**A**) ABCA12 protein (green) was localized in the cytoplasm of the upper epidermal keratinocytes (arrows) in healthy skin. (**B**) No ABCA12 immunolabeling was seen in the epidermis of patient 4. (**C**) Weak ABCA12 staining (arrows) was observed in the epidermis of patient 1. Asterisks indicate nonspecific staining in the stratum corneum. Red, nuclear counterstain. Scale bar: 10 μm. (**D–F**) By immunoelectron microscopy, ABCA12 protein (5 nm gold particles) was restricted to LGs (arrows) in the upper epidermal cell (**D**). Lamellar structures were apparent in some ABCA12-positive LGs (**E**). ABCA12-positive LGs (arrows) were observed close to the keratinocyte-cell membrane (white circles) and they fused with it to secrete their contents into the intercellular space (**F**). Scale bars: 0.2 μm. (**G**) Model of ABCA12 function in the skin. ABCA12 transports lipid into the LG, and ABCA12-positive LGs fuse with the cell membrane to secrete lipid into extracellular space to form the intercellular lipid layer. (**H**) Structure of ABCA12 protein and the 5 mutation sites (red arrows) in HI families. Dark-blue area, cell membrane; bottom of dark-blue area, cytoplasmic surface.

or homozygous state, in all patients from 4 HI families (Figure 2H). The mutations in patients were homozygous in the 2 consanguineous families and compound heterozygous in the 2 nonconsanguineous families (Figure 3). The mutations were verified in the heterozygous parents. Each of the three mutations, 1300C→T (R434X), 2021_2022delAA, and 5848C→T (R1950X), resulted in truncation of a highly conserved region of the ABCA12 protein. The deletion mutation 4158_4160delTAC led to an in-frame deletion of a highly conserved threonine residue at codon 1387 (T1387del) within the first ATP-binding domain of the ABCA12 protein (Figure 4D). A splice acceptor site mutation, IVS23-2A→G, was verified by RT-PCR in mRNA from the patient's cultured keratinocytes (Figure 4, A–C). RT-PCR products from the patient showed 2 splice pattern variants different from the normal splicing variant in which 1 mutant transcript loses a 9-bp sequence from exon 24, which results in a 3-amino acid deletion (Y1099_K1101del). These 3 amino acids are located between the transmembrane domains and are highly conserved (Figure 4D). The other mutant transcript lost a 170-bp sequence from exon 24, which led to a frameshift. All of these mutations are thought to seriously affect either the function or specific critical structures of the ABCA12 protein.

Disturbed lipid secretion in epidermis of HI patients. Morphological observations revealed extraordinarily thick stratum corneum (Figure 5A) and abnormal LG secretion in keratinocytes of the epidermis of HI patients (Figure 5, C and E). Ultrastructurally, the cytoplasm in the stratum corneum was congested with abnormal lipid-containing droplets and vacuoles that resembled immature LG-like vesicles. In the keratinocyte cytoplasm of the granular layer, no normal LGs were apparent.

Immunofluorescent staining showed that glucosylceramide, a major lipid component of LG (7, 9) and an essential component of the epidermal permeability barrier (10), was diffusely distributed throughout the epidermis of HI patients (Figure 5G); this contrasts with the restricted, intense distribution in the stratum corneum of healthy skin (Figure 5H).

Abnormal lipid secretion in keratinocytes of HI patients and recovery of ABCA12 function by corrective gene transfer. Keratinocytes from patient 1, cultured under high-Ca^{2+} conditions (2.0 mM), expressed only a small amount of mutated ABCA12 protein (Figure 6J). Culture of HI keratinocytes under high-Ca^{2+} conditions (2.0 mM) induced a large number of cells to exhibit intense glucosylceramide staining around the nuclei, and this glucosylceramide failed to localize to the periphery of the keratinocyte cytoplasm (congested pattern) (Figure 6, A and C). Conversely, culture of healthy keratinocytes in high-Ca^{2+} conditions resulted in a large proportion of cells with diffuse glucosylceramide staining throughout the cytoplasm (widely-distributed pattern) (Figure 6, B and D). This difference was most pronounced after 1 week in culture (Figure 6, C and D). Electron microscopic observation of HI keratinocytes cultured for 1 week in high-Ca^{2+} conditions revealed that LGs formed, although proper secretion of their contents was not observed (Figure 6E). This finding suggests defects in LG lipid transport. Double immunostaining for ABCA12 protein

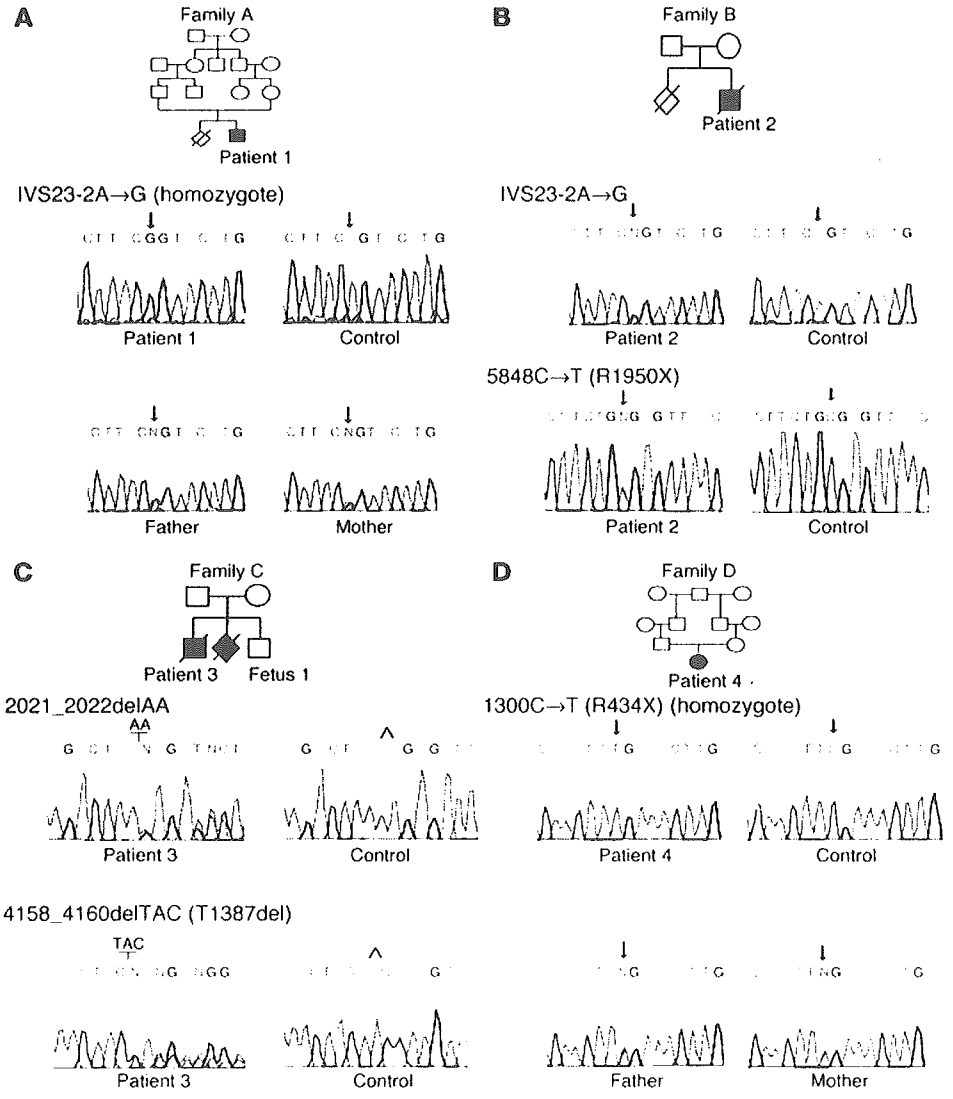

Figure 3
Families with HI and *ABCA12* mutations. (**A**) Patient 1 from family A was a homozygote for the mutation IVS23-2A→G, and both his parents were heterozygous carriers. (**B**) Patient 2 from family B was a compound heterozygote for the mutations IVS23-2A→G and 5848C→T (R1950X). (**C**) Patient 3 from family C was a compound heterozygote for the mutations 2021_2022delAA and 4158_4160delTAC (T1387del). (**D**) Patient 4 from family D was a homozygote for the mutation 1300C→T (R434X), and her 2 parents were heterozygous carriers.

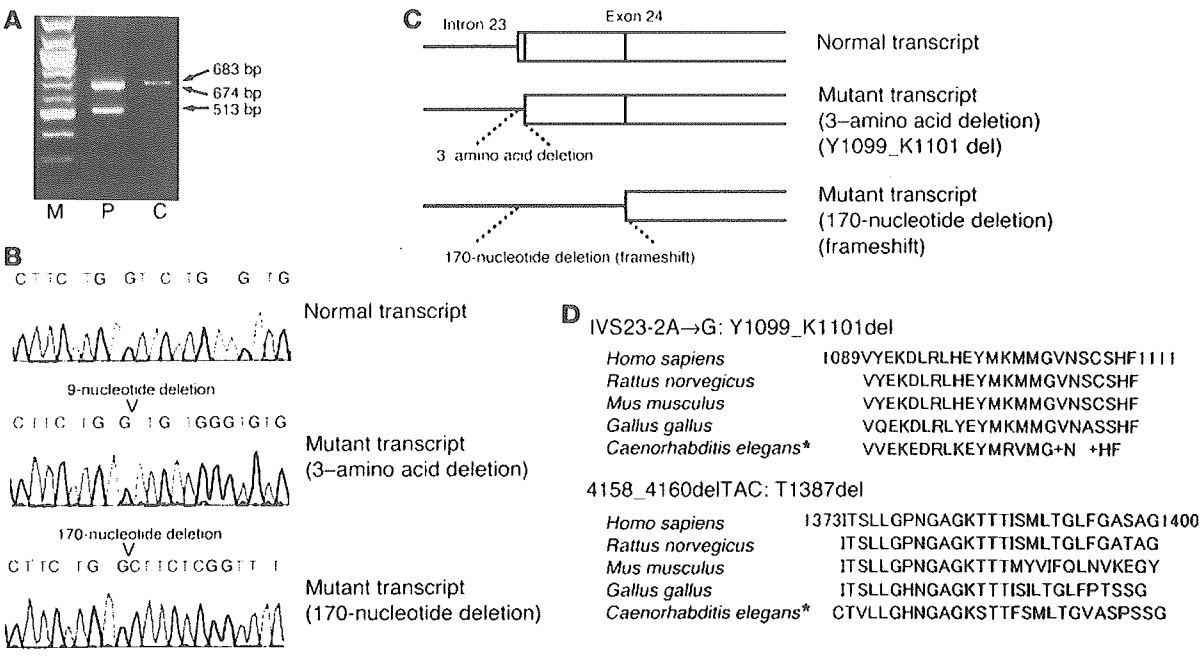

Figure 4
Verification of splice-site mutation IVS23-2A→G and conservation of residues deleted by mutations IVS23-2A→G and 4158_4160delTAC (T1387del). (**A**) RT-PCR analysis of mRNA fragments around the exon 23–24 boundary indicated that keratinocytes from patient 1 (lane P) showed 2 different mutant transcripts, 674 bp and 513 bp, which were shorter than the control transcript (683 bp) from healthy human keratinocytes (lane C). Lane M, markers. (**B**) Sequencing of the mutant transcripts and the control transcript revealed that 9 nucleotides and 170 nucleotides were deleted in mutant transcripts. (**C**) A 9-nucleotide deletion resulted in the loss of 3 amino acids from the N terminal sequence of exon 24 (Y1099_K1101del), and the 170-nucleotide deletion led to a frameshift. (**D**) ABCA12 amino acid sequence alignment shows the level of conservation in diverse species of the amino acids, Y1099_K1101 and T1387 (red characters), which were deleted by mutations in HI families. Asterisks indicate ABC (abt-4).

and glucosylceramide clearly demonstrated that, before genetic correction of ABCA12, keratinocytes from patient 1 with a low expression of mutated ABCA12 protein showed a congested glucosylceramide distribution pattern (Figure 6, J–L). After genetic correction, however, the HI patient's keratinocytes, now expressing normal ABCA12, showed a normal, widely-distributed pattern of glucosylceramide staining (Figure 6, M–O). Corrective ABCA12 gene transfer into cultured HI keratinocytes resulted in a significant increase in number of cells exhibiting the widely-distributed pattern of glucosylceramide staining from 6.98% ± 3.33% (control nontransfected patients' cells) to 16.70% ± 2.14 % (transfected patients' cells) (Student's t test, $P < 0.02$) (Figure 6P). These results clearly indicate that an ABCA12 deficiency leads to defective LG lipid transport into the intercellular space in HI patients, both in the epidermis and in cultured keratinocytes.

Discussion

An abnormal synthesis or metabolism of the LG lipid contents was previously suspected as being a possible pathogenetic mechanism underlying HI (11, 12). Here, we demonstrate that a severe ABCA12 deficiency causes defective lipid transport via LG in keratinizing epidermal cells, resulting in the HI phenotype.

The ABC transporter superfamily is one of the largest gene families, encoding a highly conserved group of proteins involved in energy-dependent active transport of a variety of substrates across membranes, including ions, amino acids, peptides, carbohydrates, and lipids (3–5, 13). ABC transporters have nucleotide-binding folds located in the cytoplasm and utilize energy from ATP to transport substrates across the cell membrane (3–5). ABC genes are widely dispersed throughout the eukaryotic genome and are highly conserved between species (6). The ABCA subfamily, of which the *ABCA12* gene is a member, comprises 12 full transporter proteins and 1 pseudogene (ABCA11). The ABCA subclass has received considerable attention (14) because mutations in these genes have been implicated in several human genetic diseases (15–19).

The ABCA1 protein is mutated in the following recessive disorders involving cholesterol and phospholipid transport: Tangier disease (MIM 205400), familial hypoalphalipoproteinemia (MIM 604091), and premature atherosclerosis, depending on the site of the mutations in the protein (17–19). The ABCA4 protein is mutated in Stargardt disease (MIM 248200) as well as in some forms of autosomal recessive retinitis pigmentosa (MIM 601718) and in the majority of cases of autosomal recessive cone-rod dystrophy (MIM 604116), depending on the mutation site or the combination of mutation types (15, 20). Heterozygous mutations in *ABCA4* have also been implicated in some cases of macular degeneration (MIM 153800) (16, 20). In a relatively mild type of congenital ichthyosis (lamellar ichthyosis type 2), 5 *ABCA12* mutations were reported in 9 families, and all 5 of these mutations were missense mutations that resulted in only 1 amino acid alteration (8). In the present series of HI patients, no *ABCA12* missense mutations were identified, and most of the defects led to severe truncation of the ABCA12 peptide, affecting important nucleotide-binding fold domains and/or transmembrane domains. The other, nontrun-

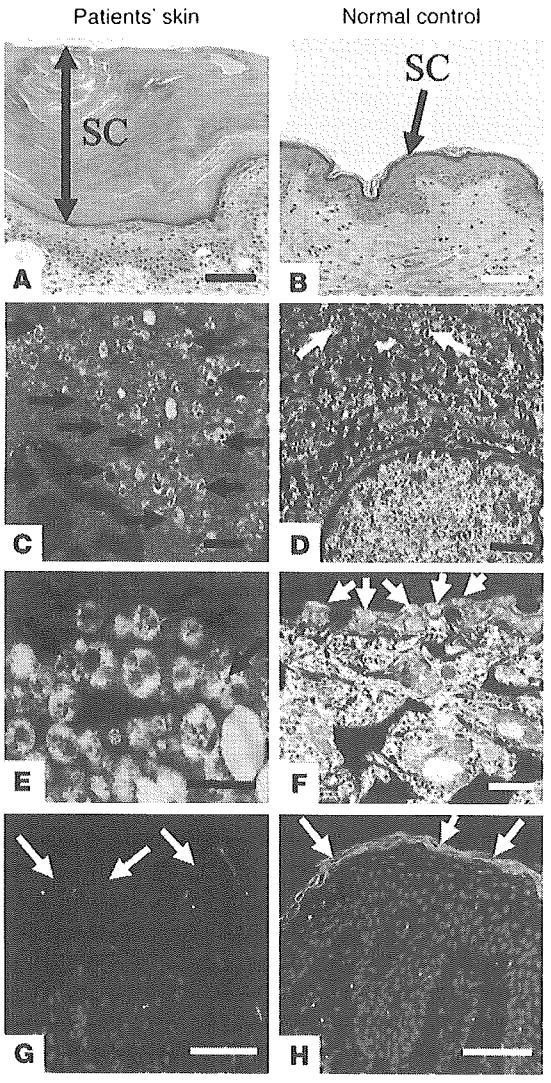

Figure 5
Extremely thick stratum corneum and severe disruption of the secretion of LGs in the ABCA12-deficient skin of the present series of HI patients. (**A**) Strikingly thick stratum corneum (SC; double arrow) in the patient's skin. (**B**) Control epidermis showing normal, stratum corneum (arrow). (**C**) By electron microscopy, LG secretion was disturbed, and many abnormal immature (lacking proper lamellar structures) LGs (arrows) were observed in the keratinocytes. (**D**) In control skin, LGs (arrows) were distributed in a gradually increasing pattern toward the plasma membrane. (**E**) Abnormal HI LGs (arrows) were localized close to the cell membrane, but not secreted. (**F**) LGs were secreted into the extracellular space (arrows). (**G**) Patient's epidermis including stratum corneum (arrows) showed diffuse staining for glucosylceramide (green), a lipid component of LGs. (**H**) Glucosylceramide staining (green) was restricted and intense in the stratum corneum (arrows) of normal skin. Red, nuclear stain. Scale bars: 50 μm (**A**, **B**, **G**, **H**); 1 μm (**C**, **D**); 0.5 μm (**E**, **F**).

cation mutations in HI were deletion mutations affecting highly conserved *ABCA12* sequences (Figure 4D). Thus, it is thought that only truncation or conserved region deletion mutations that seriously affect the function of the ABCA12 transporter protein lead to the HI phenotype. This is in contrast with diseases caused by mutations in other members of the ABCA family. Of *ABCA4* mutations causing Stargardt disease, 80% were missense, and many of these occurred in conserved domains of ABCA4 (21). Of *ABCA1* mutations resulting in Tangier disease, 60% were missense, located within the conserved domains of ABCA1 (22). In this context, *ABCA12* mutations underlying HI are unique in that these mutations are restricted to truncation or deletion mutations.

Patient 1 was homozygous for the splice acceptor site mutation IVS23-2A→G. This splice-site mutation was shown to lead to comparable amounts of 2 predicted transcripts, an inframe deletion of 3 amino acids, and a transcript with a 170-nucleotide deletion (frameshift) (Figure 4, A–C). Thus, it is still possible that patient 1 expresses some mutated ABCA12 protein. Indeed, expression of a small amount of ABCA12 protein, although mutated, was detected in the granular cells of the patient's epidermis and cultured keratinocytes by immunofluorescent staining (Figures 2C and 6J). This might have some relevance to the fact that patient 1 survived infancy and is still alive.

ABCA1 and ABCA4 are suspected transmembrane transporters for intracellular cholesterol/phospholipids (23–25) and protonated *N*-retinylidenephosphatidylethanolamines (26), respectively. *ABCA2*, *ABCA3*, and *ABCA7* mRNA levels have been reported to be upregulated by sustained cholesterol influx mediated by modified low-density lipoprotein (27, 28), suggesting that ABCA transporters are involved in transmembrane transport of endogenous lipids (23–26). Keratinocyte LGs are known lipid-transporting granules, and LG contents are secreted into the intercellular space, forming an intercellular lipid layer between the granular layer cells and keratinized cells in the stratum corneum, which is essential for the proper barrier function of human skin. Our results indicate that ABCA12 functions in the transport of endogenous lipid across the keratinocyte cell membrane into the stratum corneum intercellular space via LGs. Immunohistological and immunoelectron microscopic observations have indicated that ABCA3 is involved in lipid secretion of pulmonary surfactant in human lung alveolar type II cells (29). ABCA3 and ABCA12 are very closely related in the ABCA subfamily phylogenetic tree (30). It is interesting that the functions of both ABCA3 and ABCA12 are involved in alveolar surfactant and stratum corneum lipid secretion, respectively. This suggests that these 2 transporter systems are evolutionary adaptations to aid the respiratory system and the integument in a dry environment, developed as vertebrates left the aquatic environment and began terrestrial lives. HI skin that harbors serious defects in ABCA12 highlights the important role(s) of epidermal lipid transport in adapting human skin to a terrestrial, dry environment.

HI is one of the most severe of all genodermatoses and has a very poor prognosis. Thus, parents' request for prenatal diagnosis is to be taken seriously and with care. However, to our knowledge, the causative gene was not identified until now. For the last 20 years, prenatal diagnoses have only been performed by electron microscopic observation of fetal skin biopsy at a late stage of pregnancy (19–23 weeks estimated gestational age) (31–33). In this report, we have identified the causative gene in HI, which now makes possible DNA-based prenatal diagnosis using chorionic villus or amniotic fluid sampling at an earlier stage of pregnancy, with a lower procedural risk and a reduced burden on prospective mothers, similar to that of screening for other severe genetic disorders, including keratinization disorders (34). Furthermore, we have performed correc-

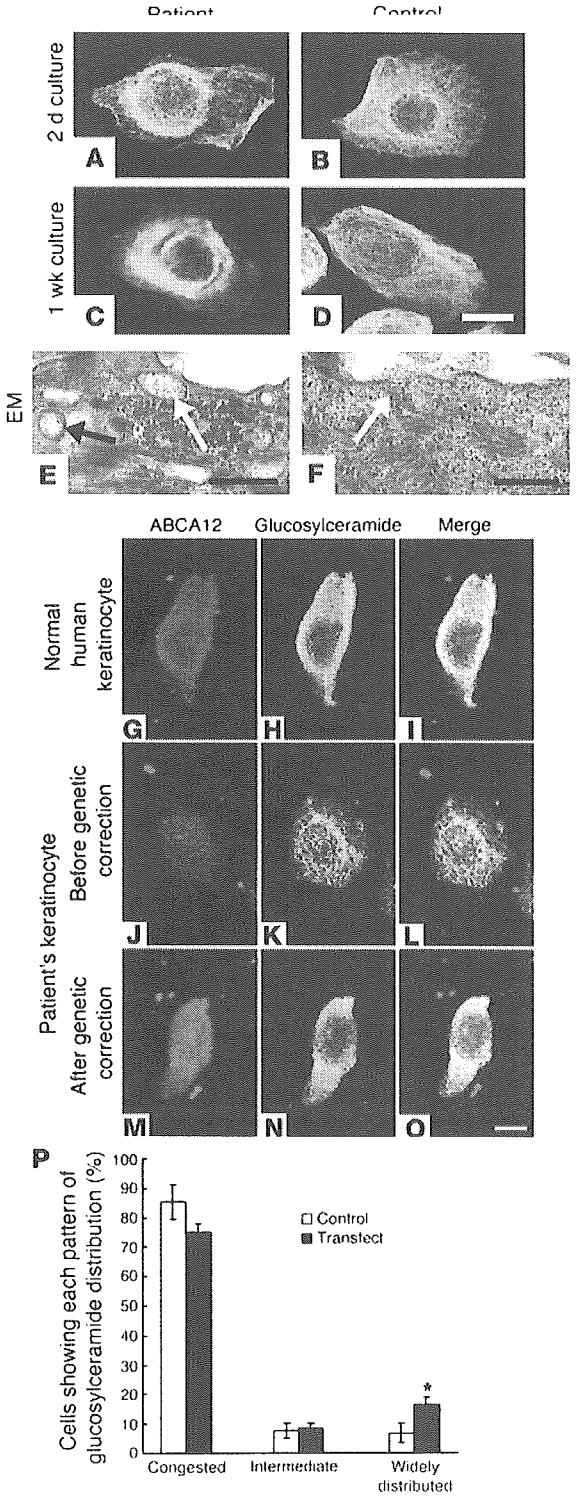

Figure 6
Cultured HI keratinocytes carrying *ABCA12* mutations showed abnormal congestion of lipid, and this phenotype was recovered by corrective *ABCA12* gene transfer. (**A–D**) HI keratinocytes cultured in high Ca^{2+} conditions showed that glucosylceramide, a major component of LG lipid, was distributed densely around the nuclei (in a congested pattern) (green, FITC). Control normal human keratinocytes showed a widely distributed, diffuse glucosylceramide staining pattern. (**E**) Electron microscopic (EM) observation revealed, in cultured HI keratinocytes, that apparently amorphous, electron lucent LG-like structures (arrows) formed, but were not secreted. (**F**) Normal secretion of LG contents (arrow) in a control keratinocyte. (**G–O**) Before genetic correction, an HI patient cell showed weak ABCA12 immunostaining (red, TRITC) and a congested pattern of glucosylceramide staining (green, FITC) (**J–L**). After genetic correction, an HI patient cell demonstrated stronger ABCA12 labeling (red) and a normal distribution pattern of glucosylceramide (green) (**M–O**), similar to those of a normal human keratinocyte (**G–I**). (**P**) Corrective gene transfer resulted in a statistically significant increase in the number of cells with completely normal, widely distributed glucosylceramide patterns. $^*P < 0.02$, Student's *t* test. Scale bars: 10 μm (**A–D**, **G–O**); 0.5 μm (**E**, **F**).

tive gene transfer in HI keratinocytes and succeeded in obtaining phenotypic rescue of a patient's cultured keratinocytes. These data provide significant clues that establish a strategic approach to HI gene therapy treatment. We believe that the genetic information presented in this study will be highly beneficial to our understanding of HI pathogenesis and in optimizing HI patient diagnosis, genetic counseling, care, and treatment.

Methods

Patients and families. Four HI patients, patients 1–4, and 1 affected fetus, fetus 1 (4 males, 1 female), from 4 independent families, families A–D, showed a serious collapse in the keratinized skin barrier (Figure 1). Family A and family D were consanguineous (marriage of first cousins). All the patients showed severe hyperkeratosis at birth and presented with generalized, thick scales over their entire body surface with the presence of marked fissuring. Severe ectropion, eclabium, and malformed pinnae were apparent in all cases. Patient 2 from family B died 3 days after birth. Patient 3 from family C died 15 days after birth, and an affected fetus from family C was terminated at the parents' request after a positive prenatal diagnostic skin test (33). After written, informed consent was obtained, blood samples were collected from each participating family member, and skin biopsy or autopsy specimens were obtained from the patients and the affected fetus. The study was given appropriate ethical approval by the Ethics Committee at Hokkaido University Graduate School of Medicine.

Mutation screening. Mutation analysis was performed in patients, an affected fetus, and other family members in the 4 families, as far as DNA samples would allow. Briefly, genomic DNA isolated from peripheral blood was subjected to PCR amplification, followed by direct automated sequencing using an ABI PRISM 3100 genetic analyzer (Applied Biosystems). Oligonucleotide primers and PCR conditions used for amplification of exons 1–53 of *ABCA12* were originally derived from the report by Lefèvre et al. (8) and were partially modified for the present study. The entire coding region, including the exon/intron boundaries for both forward and reverse strands from all patients, family members, and controls, were sequenced. No mutations were found in 100 control alleles from the Japanese population.

Verification of the splice acceptor site mutation. In order to verify the splice acceptor site mutation IVS23-2A→G, RT-PCR amplification of mRNA spanning the exon 23–24 boundary was performed using mRNA samples from cultured HI keratinocytes (see below). After RT-PCR amplification, direct sequencing of the products was performed.

Establishment of HI keratinocyte cell culture. A skin sample from patient 1 was processed for primary keratinocyte culture, and cells were grown according to standard procedures in defined keratinocyte serum-free medium (Invitrogen Corp.). Cultures were grown for several passages in low-Ca^{2+} (0.09 mM) conditions and then switched to high-Ca^{2+} (2.0 mM) conditions.

RT-PCR of ABCA12 mRNA. RT-PCR of ABCA12 mRNA was performed with Superscript 2 (Invitrogen Corp.) following the manufacturer's

instructions. Specific primers for PCR amplification were as follows: forward 5′-GAATTGCAAACTGGAAGGAACTCCC-3′ and reverse 5′-GAGTCAGCTAGGATTAGACAGC-3′. These primers were used for amplification of a 683-bp fragment around exon 23–24 boundary of normal cDNA.

Real time-PCR. For quantitative analysis of *ABCA12* expression levels, total RNA extracted was subjected to real-time RT-PCR using the ABI PRISM 7000 sequence detection system (Applied Biosystems). Specific primers/probes for human *ABCA12*, TaqMan Gene Expression Assay (HS00292421; Applied Biosystems) were used. Differences between the mean *CT* values of *ABCA12* and those of *GAPDH* were calculated as $\Delta CT_{sample} = CT_{ABCA12} - CT_{GAPDH}$ and those of the ΔCT for the cultured keratinocytes in the low Ca^{2+} condition as $(\Delta CT_{calibrator} = CT_{ABCA12} - CT_{GAPDH})$. Final results, the sample-calibrator ratio, expressed as *n*-fold differences in *ABCA12* expression were determined by $2^{-(\Delta CTsample - \Delta CTcalibrator)}$.

Cloning of ABCA12 and corrective gene transfer of HI keratinocytes. Using human keratinocyte cDNA as a template, overlapping clones of human *ABCA12* cDNA were amplified by PCR. A composite full-length cDNA was constructed, subjected to nucleotide sequencing, and subcloned into a pCMV-tag4B vector (Stratagene). The expression plasmid pCMV-tag4B-ABCA12 was transfected into HI keratinocytes using Lipofectamine reagent (Invitrogen Corp.) according to the manufacturer's recommendation. As a control, pCMV-tag4B was transfected into the cells. The transfected cells and control cells from patient 1 were stained with anti-glucosylceramide antibody, and the number of keratinocytes showing the 3 distinct types of glucosylceramide distribution patterns — congested, intermediate, and widely distributed — were assessed and calculated by 1 observer after viewing under a confocal laser scanning microscope, the Olympus Fluoview, FV300 confocal microscope (Olympus).

Morphological observation. Skin biopsy samples or cultured keratinocytes were fixed in 2% glutaraldehyde solution, postfixed in 1% OsO4, dehydrated, and processed for conventional electron microscopic observation.

Antibodies. Polyclonal anti-ABCA12 antibody was raised in rabbits using a 14-amino acid sequence synthetic peptide (residues 2567-2580) derived from the ABCA12 sequence (NM 173076) as the immunogen. The other primary antibody was mouse monoclonal anti-ceramide antibody (Alexis Biochemicals).

Immunofluorescent labeling. Immunofluorescent labeling was performed on frozen tissue sections and keratinocyte cultures as previously described (35). Fluorescent labeling was performed with FITC-conjugated secondary antibodies, followed by 10 μg/ml propidium iodide (Sigma-Aldrich) to counterstain nuclei. For double labeling, fluorescent labeling was performed with a TRITC-conjugated secondary antibody for the anti-ABCA12 antibody. The stained samples were observed under a confocal laser scanning microscope.

Postembedding immunogold electron microscopy. Normal human skin samples were obtained from skin surgical operations under fully informed consent and were processed for postembedding immunoelectron microscopy as previously described (36). Cyrofixed, cryosubstituted samples were embedded in Lowicryl K11M resin (Electron Microscopy Sciences). Ultrathin sections were cut and incubated with anti-ABCA12 antibody, a secondary linker antibody, and a 5-nm gold-conjugated antibody for immunogold labeling.

Acknowledgments

We thank members of the patients' families for their cooperation; Peter M. Elias for helpful discussion; Sadae Egawa, Haruhiko Sago, Judith Allanson, and Linlea Armstrong for their help; and Akari Nagasaki and Megumi Sato for their technical assistance. This work was supported in part by a Grant-in-Aid from the Ministry of Education, Science, Sports, and Culture of Japan (Kiban B 16390312; to M. Akiyama).

Received for publication February 23, 2005, and accepted in revised form April 12, 2005.

Address correspondence to: Masashi Akiyama, Department of Dermatology, Hokkaido University Graduate School of Medicine, N15 W 7, Sapporo 060-8638, Japan. Phone: 81-11-716-1161; Fax: 81-11-706-7820; E-mail: akiyama@med.hokudai.ac.jp.

1. Williams, M.L., and Elias, P.M. 1987.Genetically transmitted, generalized disorders of cornification; the ichthyoses. *Dermatol. Clin.* **5**:155–178.
2. Judge, M.R., McLean, W.H.I., and Munro, C.S. 2004. Disorders of keratinization. In *Rook's textbook of dermatology.* 7th edition. T. Burns, S. Breathnach, N. Cox, and C. Griffiths, editors. Blackwell Publishers. Oxford, United Kingdom. 34.1–34.111.
3. Allikmets, R., Gerrard, B., Hutchinson, A., and Dean, M. 1996. Characterization of the human ABC superfamily: isolation and mapping of 21 new genes using the expressed sequence tags database. *Hum. Mol. Genet.* **5**:1649–1655.
4. Dean, M., Rzhetsky, A., and Allikmets, R. 2001. The human ATP-binding cassette (ABC) transporter superfamily. *Genome Res.* **11**:1156–1166.
5. Borst, P., and Elferink, R.O. 2002. Mammalian ABC transporters in health and disease. *Annu. Rev. Biochem.* **71**:537–592.
6. Peelman, F., et al. 2003. Characterization of the ABCA transporter subfamily: identification of prokaryotic and eukaryotic members, phylogeny and topology. *J. Mol. Biol.* **325**:259–274.
7. Ishida-Yamamoto, A., et al. 2004. Epidermal lamellar granules transport different cargoes as distinct aggregates. *J. Invest. Dermatol.* **122**:1137–1144.
8. Lefèvre, C., et al. 2003. Mutations in the transporter ABCA12 are associated with lamellar ichthyosis type 2. *Hum. Mol. Genet.* **12**:2369–2378.
9. Vielhaber, G., et al. 2001. Localization of ceramide and glucosylceramide in human epidermis by immunogold electron microscopy. *J. Invest. Dermatol.* **117**:1126–1136.
10. Holleran, W.M., et al. 1993. Processing of epidermal glucosylceramides is required for optimal mammalian cutaneous permeability barrier function. *J. Clin. Invest.* **91**:1656–1664.
11. Dale, B.A., et al. 1990. Heterogeneity in harlequin ichthyosis, an inborn error of epidermal keratinization: variable morphology and structural protein expression and a defect in lamellar granules. *J. Invest. Dermatol.* **94**:6–18.
12. Milner, M.E., O'Guin, W.M., Holbrook, K.A., and Dale, B.A. 1992. Abnormal lamellar granules in harlequin ichthyosis. *J. Invest. Dermatol.* **99**:824–829.
13. Higgins, C.F. 1992. ABC transporters: from microorganisms to man. *Annu. Rev. Cell Biol.* **8**:67–113.
14. Klein, I., Sarkadi, B., and Varadi, A. 1999. An inventory of the human ABC proteins. *Biochim. Biophys. Acta.* **1461**:237–262.
15. Allikmets, R., et al. 1997. A photoreceptor cell-specific ATP-binding transporter gene (ABCR) is mutated in recessive Stargardt macular dystrophy. *Nat. Genet.* **15**:236–246.
16. Allikmets, R., et al. 1997. Mutation of the Stargardt disease gene (ABCR) in age-related macular degeneration. *Science.* **277**:1805–1807.
17. Brooks-Wilson, A., et al. 1999. Mutations in ABC1 in Tangier disease and familial high-density lipoprotein deficiency. *Nat. Genet.* **22**:336–345.
18. Rust, S., et al. 1999. Tangier disease is caused by mutations in the gene encoding ATP-binding cassette transporter 1. *Nat. Genet.* **22**:352–355.
19. Oram, J.F. 2002. Molecular basis of cholesterol homeostasis: lessons from Tangier disease and ABCA1. *Trends Mol. Med.* **8**:168–173.
20. Allikmets, R. 2000. Simple and complex ABCR: genetic predisposition to retinal disease. *Am. J. Hum. Genet.* **67**:793–799.
21. Lewis, R.A., et al. 1999. Genotype-phenotype analysis of a photoreceptor-specific ATP-binding cassette transporter gene, ABCR, in Stargardt disease. *Am. J. Hum. Genet.* **64**:422–434.
22. Huang, W., et al. 2001. Novel mutations in ABCA1 gene in Japanese patients with Tangier disease and familial high density lipoprotein deficiency with coronary heart disease. *Biochim. Biophys. Acta* **1537**:71–78.
23. Hayden, M.R., et al. 2000. Cholesterol efflux regulatory protein, Tangier disease and familial high-density lipoprotein deficiency. *Curr. Opin. Lipidol.* **11**:117–122.
24. Orso, E., et al. 2000. Transport of lipids from Golgi to plasma membrane is defective in Tangier disease patients and Abc1-deficient mice. *Nat. Genet.* **24**:192–196.
25. Schmitz, G., and Langmann, T. 2001. Structure, function and regulation of the ABC1 gene product. *Curr. Opin. Lipidol.* **12**:129–140.
26. Weng, J., et al. 1999. Insights into the function of Rim protein in photoreceptors and etiology of Stargardt's disease from the phenotype in abcr knockout mice. *Cell.* **98**:13–23.
27. Klucken, J., et al. 2000. ABCG1 (ABC8), the human homolog of the Drosophila white gene, is a regulator of macrophage cholesterol and phospholipid transport. *Proc. Natl. Acad. Sci. U. S. A.* **97**:817–822.
28. Kaminski, W.E., et al. 2001. Complete coding sequence, promoter region, and genomic structure

of the human ABCA2 gene and evidence for sterol-dependent regulation in macrophages. *Biochem. Biophys. Res. Commun.* **281**:249–258.
29. Yamano, G., et al. 2001. ABCA3 is a lamellar body membrane protein in human lung alveolar type II cells. *FEBS Lett.* **508**:221–225.
30. Annilo, T., et al. 2002. Identification and characterization of a novel ABCA subfamily member, ABCA12, located in the lamellar ichthyosis region on 2q34. *Cytogenet. Genome Res.* **98**:169–176.
31. Blanchet-Bardon, C., et al. 1983. Prenatal diagnosis of harlequin fetus [letter]. *Lancet.* **1**:132.
32. Akiyama, M., Kim, D.-K., Main, D.M., Otto, C.E., and Holbrook, K.A. 1994. Characteristic morphologic abnormality of harlequin ichthyosis detected in amniotic fluid cells. *J. Invest. Dermatol.* **102**:210–213.
33. Akiyama, M., Suzumori, K., and Shimizu, H. 1999. Prenatal diagnosis of harlequin ichthyosis by the examinations of keratinized hair canals and amniotic fluid cells at 19 weeks' estimated gestational age. *Prenat. Diagn.* **19**:167–171.
34. Tsuji-Abe, Y., et al. 2004. DNA-based prenatal exclusion of bullous congenital ichthyosiform erythroderma at the early stage, 10-11 weeks' of pregnancy in two consequent siblings. *J. Am. Acad. Dermatol.* **51**:1008–1011.
35. Akiyama, M., et al. 1999. Periderm cells form cornified cell envelope in their regression process during human epidermal development. *J. Invest. Dermatol.* **112**:903–909.
36. Shimizu, H., McDonald, J.N., Kennedy, A.R., and Eady, R.A.J. 1989. Demonstration of intra- and extra-cellular localization of bullous pemphigoid antigen using cryofixation and freeze substitution for postembedding immuno-electron microscopy. *Arch. Dermatol. Res.* **281**:443–448.

DOI 10.1111/j.1365-2133.2005.06598.x

Ichthyosis bullosa of Siemens: its correct diagnosis facilitated by molecular genetic testing

M. Akiyama, Y. Tsuji-Abe, M. Yanagihara,* K. Nakajima,† H. Kodama,† M. Yaosaka, M. Abe, D. Sawamura and H. Shimizu

Department of Dermatology, Hokkaido University Graduate School of Medicine, N15 W7, Sapporo 060-8638, Japan
**Department of Dermatology, Kanazawa Medical University School of Medicine, Ishikawa, Japan*
†Department of Dermatology, Kochi Medical School, Nankoku, Japan

Correspondence
Masashi Akiyama.
E-mail: akiyama@med.hokudai.ac.jp

Accepted for publication
20 December 2004

Key words:
bullous congenital ichthyosiform erythroderma, epidermolytic hyperkeratosis, genodermatosis, ichthyosis bullosa of Siemens, intermediate filaments

Conflicts of interest:
None declared.

Summary

Ichthyosis bullosa of Siemens (IBS, MIM 146800) is a unique congenital ichthyosis characterized by mild epidermal hyperkeratosis over flexural areas, blister formation and the development of superficially denuded areas of hyperkeratotic skin. It is clinically difficult to distinguish severe IBS from mild bullous congenital ichthyosiform erythroderma (BCIE, MIM 113800). In the current literature, 19 IBS families with keratin 2e (K2e) mutations have been reported, despite only five IBS families having been reported before the first identification of K2e mutation in 1994. We studied four patients from three Japanese IBS families. They had previously been misdiagnosed as having BCIE before the correct diagnosis was made after mutation detection. To detect the pathogenic mutations, we performed direct sequencing of the entire coding regions of KRT2E encoding K2e in the patients and healthy family members. K2e mutations, a 1469T → C transition (L490P) and a 1477G → A transition (E493K) within the conserved 2B helix termination motif of the rod domain were detected in the families and the definite diagnosis of IBS was made in the four cases. The present results indicate that IBS is not such a rare entity as was previously thought, and accurate diagnosis is now available by mutation analysis.

Ichthyosis bullosa of Siemens (IBS, MIM 146800) is an autosomal dominant hereditary keratinization disorder which shows similar, but milder, clinical and histopathological findings to those in bullous congenital ichthyosiform erythroderma (BCIE, MIM 113800).[1] In 1994, keratin 2e (K2e) mutations were identified as causative in patients with IBS.[2–4] It has been thought that IBS could be distinguished from BCIE by the milder clinical manifestations, the absence of erythroderma, the presence of superficial denuded areas over hyperkeratotic skin (the *Mauserung* phenomenon), and by the characteristic distribution of hyperkeratosis. Histologically, the epidermolytic hyperkeratosis in IBS is confined to the granular and upper spinous layers with intracorneal blister formation.[1]

Despite these characteristic findings in IBS, however, it is very difficult to distinguish severe cases of IBS from mild cases of BCIE.[2,5,6] It is feasible that some patients with IBS may have been misdiagnosed as having mild BCIE, partly because IBS was thought to be an extremely rare condition. In this report, we present four IBS patients from three families who were clinically misdiagnosed for years as having BCIE, but who were finally given the correct diagnosis of IBS after the detection of K2e gene mutations.

Case reports

We present four patients from three independent, unrelated families of Japanese origin. All the patients were both clinically and histopathologically misdiagnosed for years as having BCIE.

Family 1

Patient 1, a 9-year-old girl, had had blister formation over her whole body since 1 year of age. Physical examination revealed that she had dark to light grey hyperkeratosis covering the extremities and buttocks (Fig. 1a). The palms and soles were spared. Blisters and superficial denuded areas were noted on the extremities (Fig. 1b). No other family members, including her two brothers, showed any skin symptoms.

Family 2

Patient 2, a 56-year-old woman, had had blisters on her extremities since 8 months of age. Since infancy, hyperkeratosis had been apparent over the whole body. Physical examination

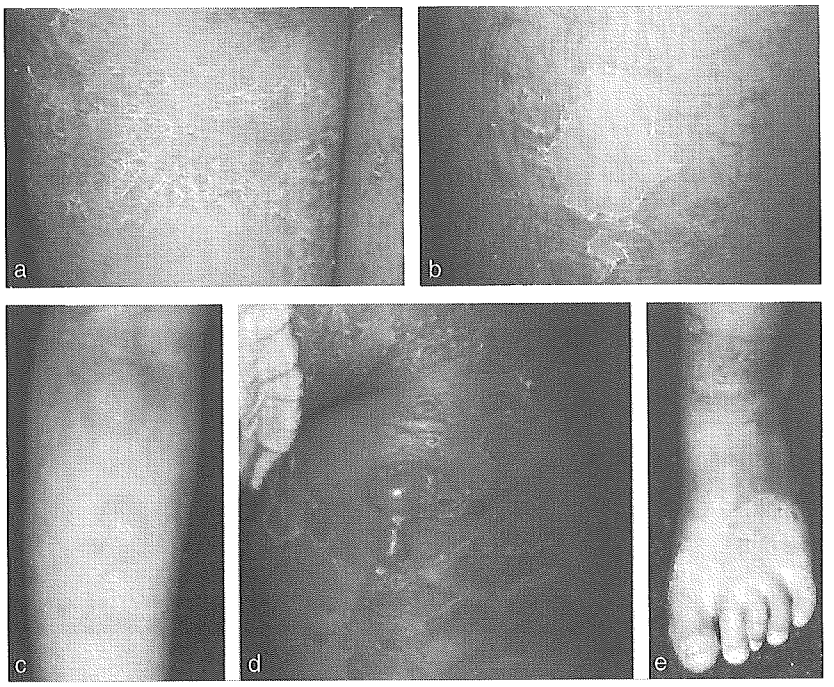

Fig 1. Clinical features of the patients with ichthyosis bullosa of Siemens. Hyperkeratosis on the flexor thigh (a) and a superficial denuded area on the lower leg (b) of patient 1. Annular erythema with scales on the forearm of patient 2 (c). Blisters and scales on the erythematous skin of the leg (d) and hyperkeratosis and a superficial denuded area on the dorsum of the foot (e) of patient 4.

revealed that she had fine, grey scales covering the extremities and buttocks. Superficial denuded areas were noted on the extremities. Annular erythema was also noted on the extremities (Fig. 1c) and the trunk. The palms and soles were spared. Patient 3, her son, was a 28-year-old man showing similar skin symptoms. When he was 3 months old, blisters and thick scales were seen on his trunk and extremities. Physical examination revealed that he had dark grey hyperkeratosis covering the extremities and buttocks. Scales were prominent on the elbows, knees, ankle and wrist joints and axillae, although the palms and soles were spared. Small blisters were noted on the extremities.

Family 3

Patient 4, a 3-year-old boy, had had a history of blistering on the extremities since he was 1 month old. Physical examination revealed that he had dark grey hyperkeratosis and scales mainly covering the extensor side of his extremities and the buttocks. Blisters and superficially denuded areas were noted in the hyperkeratotic plaques on the extremities (Fig. 1d,e). The palms and soles were spared. His father, paternal grandmother and aunt showed similar symptoms.

Mutation detection

DNA was isolated by standard methods from the peripheral blood of the patients and unaffected family members. The coding regions of the K2e gene (KRT2E) were amplified by polymerase chain reaction (PCR) using genomic DNA as a template. We employed oligonucleotide primers for amplification of all nine KRT2E exons, as reported elsewhere.[5] Specifically, the sense primer 5′-ACCTAACACTCCCAGGGCCA-3′ and antisense primer 5′-CCCCATTCTCTGCTTTCCCT-3′ were used for amplification of exon 7. All PCR products were sequenced in an ABI 310 automated sequencer.

Direct sequencing of exon 7 of KRT2E disclosed a T → C transition at nucleotide position 1469 in patient 1 from family 1 (Fig. 2a). This nucleotide substitution resulted in the change of a codon from leucine to proline (CTG → CCG), and the mutation was designated as L490P, which has previously been reported to be pathogenic in IBS.[3]

Direct sequencing of exon 7 disclosed a G → A transition at nucleotide position 1477 in patients 2 and 3 from family 2 and patient 4 from family 3 (Fig. 2b,c). This nucleotide substitution resulted in the change of a codon for glutaminc acid to lysine (GAG → AAG), and the mutation was designated as E493K, which has previously been reported in IBS.[2–4,7–9] These mutations were not found by direct sequencing in DNA samples from any other healthy family members.

Ultrastructure and distribution of keratin 2e and other keratinization-associated molecules

Electron microscopic observations of skin biopsy specimens revealed a disrupted keratin filament network and clumped keratin filaments only in the granular cells and in the spinous cells just below the granular layer.

Immunofluorescence labelling was performed as described previously.[10] The stained sections were observed using a confocal laser scanning microscope. Immunofluorescence labelling with anti-K2e antibody (Progen Biotechnik GmbH, Heidelberg, Germany) showed that K2e was expressed in the granular layers and lower down into the spinous layers in the epidermis of patient 1, whereas K2e was distributed only in the uppermost spinous and the granular layers in normal

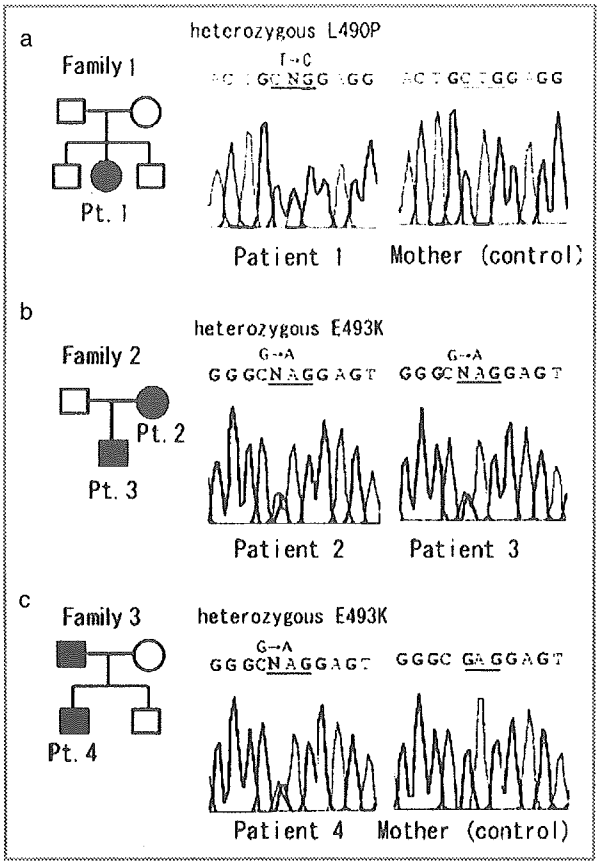

Fig 2. Pedigrees of the families and KRT2E sequences from the patients and normal controls. Patient 1 from family 1 (a) showed a 1469T → C transition. Patients 2 and 3 from family 2 (b) and patient 4 from family 3 (c) had a 1477G → A transition. Affected individuals are indicated by black symbols.

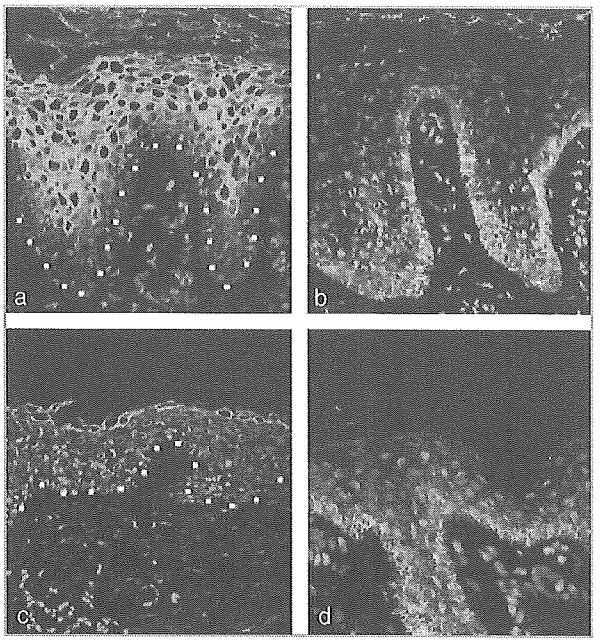

Fig 3. Immunofluorescence labelling for keratin 2e (K2e) revealed an abnormally broadened K2e-positive zone in the upper epidermis of the patient's skin (a), compared with normal control skin (c) (dotted line, basement membrane zone). A comparison with keratin 5 (K5) immunostaining (b,d) indicates clear K2e expression in the upper spinous layers in the patient's epidermis. (a,b) Patient epidermis; (c,d) normal control epidermis; (a,c) K2e staining; (b,d) K5 staining. K2e or K5, fluorescein isothiocyanate (green); nuclei, propidium iodide (red). Original magnification ×30.

control skin (Fig. 3). Keratin 1 (K1), keratin 5 (K5), keratin 10 (K10), involucrin and loricrin were all normally distributed even in the patient's epidermis.

Discussion

In all members of the keratin protein family, the helix boundary motifs are highly conserved regions of approximately 20 amino acids located at the beginning and end of the central coiled-coil rod domain, which have been implicated in molecular overlapping interactions as part of the formation of 10-nm filaments from dimers comprising both type I acidic and a type II basic-neutral keratins.[11] Single amino acid alterations by point mutation in these essential, helix boundary motifs frequently cause a disease phenotype in the majority of the keratin diseases (Human Intermediate Filament Mutation Database, http://www.interfil.org). The same is true in IBS, and all the causative mutations have been identified in the K2e protein helix initiation or termination motifs. We describe three Japanese families with IBS. One family had the mutation L490P and the other two families had the mutation E493K in the 2B helix termination motif of K2e.

In the human epidermis, K1 and K10 expression occurs in the suprabasal layers, replacing K5 and keratin 14 as cells differentiate.[12] K2e is expressed somewhat later in keratinocyte differentiation as keratinocytes approach the granular layer. In the present study, by immunofluorescence, a greater thickness of the zone of K2e-positive keratinocytes was seen in the patient's epidermis. Costaining with anti-K2e and anti-K5 antibodies clearly demonstrated that K2e expression was occurring lower down into the spinous layers than in normal epidermis. However, ultrastructurally, clumped keratin filaments were restricted to the cytoplasm of granular layer cells and the uppermost spinous layer cells. These findings suggested that, in the patient's epidermis, granular degeneration occurred only in the uppermost spinous and granular layers, although hyperkeratosis in the lesional epidermis resulted in a secondary overexpression of K2e in the spinous layers of the patient's epidermis.

The palms and soles were completely spared in all the present patients. In IBS the palms and soles are always spared, while they may be mildly scaly in BCIE patients with K10 mutations. BCIE patients with K1 mutations generally have severe palmoplantar keratoderma. Thus, the presence of and type of palmoplantar keratoderma might be a useful diagnostic indicator for IBS and BCIE.

Since 1994, when the causative genetic defects for IBS were first identified as mutations in KRT2E coding K2e,

